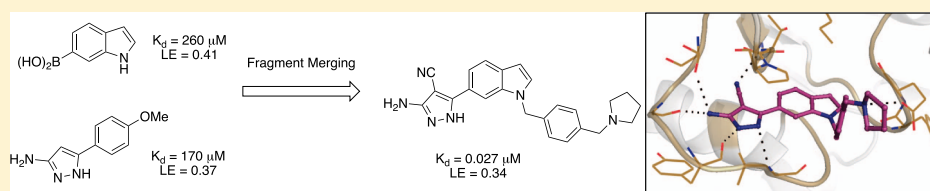


Development of Inhibitors against *Mycobacterium abscessus* tRNA (m¹G37) Methyltransferase (TrmD) Using Fragment-Based ApproachesAndrew J. Whitehouse,[†] Sherine E. Thomas,[‡] Karen P. Brown,^{§,||} Alexander Fanourakis,[†] Daniel S.-H. Chan,[†] M. Daben J. Libardo,[⊥] Vitor Mendes,[‡] Helena I. M. Boshoff,[⊥] R. Andres Floto,^{§,||} Chris Abell,^{*,†,||} Tom L. Blundell,^{*,‡} and Anthony G. Coyne^{*,†,||}[†]Department of Chemistry, University of Cambridge, Lensfield Road, Cambridge CB2 1EW, U.K.[‡]Department of Biochemistry, University of Cambridge, Tennis Court Road, Cambridge CB2 1GA, U.K.[§]Molecular Immunity Unit, Department of Medicine, MRC Laboratory of Molecular Biology, University of Cambridge, Francis Crick Avenue, Cambridge Biomedical Campus, Cambridge CB2 0QH, U.K.^{||}Cambridge Centre for Lung Infection, Royal Papworth Hospital, Cambridge CB23 3RE, U.K.[⊥]Tuberculosis Research Section, Laboratory of Clinical Immunology and Microbiology, National Institute of Allergy and Infectious Disease, National Institutes of Health, 9000 Rockville Pike, Bethesda, Maryland 20892, United States

Supporting Information



ABSTRACT: *Mycobacterium abscessus* (*Mab*) is a rapidly growing species of multidrug-resistant nontuberculous mycobacteria that has emerged as a growing threat to individuals with cystic fibrosis and other pre-existing chronic lung diseases. *Mab* pulmonary infections are difficult, or sometimes impossible, to treat and result in accelerated lung function decline and premature death. There is therefore an urgent need to develop novel antibiotics with improved efficacy. tRNA (m¹G37) methyltransferase (TrmD) is a promising target for novel antibiotics. It is essential in *Mab* and other mycobacteria, improving reading frame maintenance on the ribosome to prevent frameshift errors. In this work, a fragment-based approach was employed with the merging of two fragments bound to the active site, followed by structure-guided elaboration to design potent nanomolar inhibitors against *Mab* TrmD. Several of these compounds exhibit promising activity against mycobacterial species, including *Mycobacterium tuberculosis* and *Mycobacterium leprae* in addition to *Mab*, supporting the use of TrmD as a target for the development of antimycobacterial compounds.

INTRODUCTION

Mycobacterium abscessus (*Mab*) is an opportunistic human pathogen responsible for a wide range of lung, skin, and soft tissue infections. Although acquisition was thought to occur through environmental exposure (from soil and/or water), it has become apparent that indirect person-to-person transmission may be an important route of infection in cystic fibrosis (CF) patients (via fomite or long-lived infectious aerosol spread).^{1,2} In CF patients, *Mab* infection results in accelerated inflammatory lung damage and impaired quality and quantity of life.^{3–5} *Mab* is challenging to treat because of its unique combination of drug-modifying enzymes, high number of efflux pumps, and genetic polymorphism of target genes, in addition to its complex and impermeable multilayered cell envelope. As a result, *Mab* possesses both intrinsic and acquired resistance to currently available antibiotics⁶ and is therefore currently difficult or sometimes impossible to treat.⁵ Consequently, there is an acute

need for novel antibiotics with improved efficacy against *Mab* infection.

tRNA (m¹G37) methyltransferase (TrmD), a member of the SpoU-TrmD (SPOUT) RNA methyltransferase family, catalyzes the transfer of a methyl group from S-adenosyl methionine (SAM) to the N¹ position of guanosine 37 in bacterial tRNA when preceded by another guanosine in the sequence.⁷ The addition of this marker immediately adjacent to the anticodon acts to improve reading frame maintenance on the ribosome, preventing frameshift errors that would result in truncated and inactive peptides.⁸ TrmD has been shown to be essential for growth in a range of bacterial species from *Staphylococcus aureus* and *Pseudomonas aeruginosa* to mycobacteria, including *Mycobacterium tuberculosis* (*Mtb*) and *Mab*.^{9–12}

Received: May 17, 2019

Published: July 8, 2019

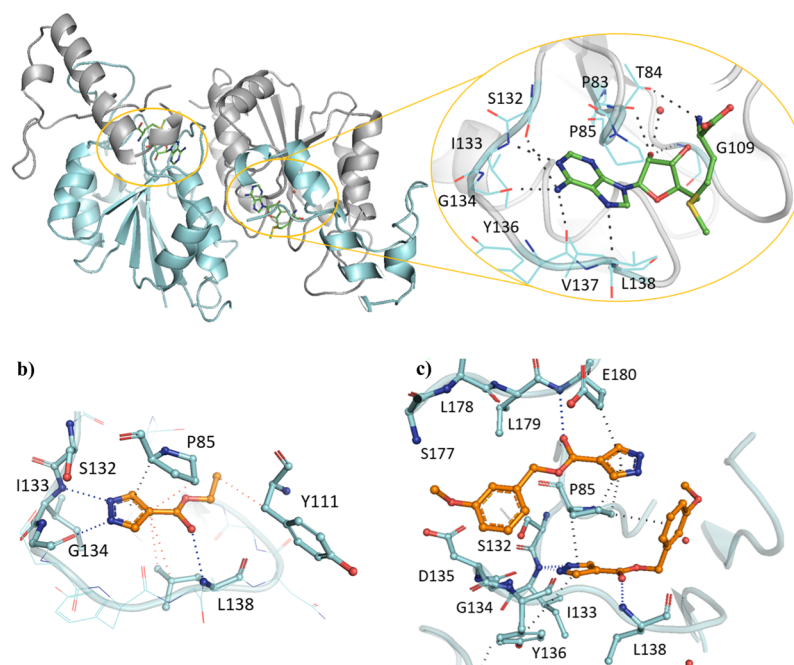


Figure 1. (a) X-ray crystal structures of *Mab* TrmD in complex with SAM (PDB code 6NW6),¹² illustrating both the whole dimer (individual protomers in blue/gray) with the positions of the active sites highlighted and one of the active sites in detail, and *Mab* TrmD in complex with (b) **1** (PDB code 6QOS)¹² and (c) **7** (PDB code 6QRE), illustrating one of the active sites.

The X-ray crystal structure of *Mab* TrmD shows a fold consistent with that of previously described TrmD enzymes,^{13–15} with a homodimeric structure exhibiting deep trefoil knots for SAM binding in two symmetry-related sites. These sites are formed by contributions from the N- and C-terminal domains of alternate subunits, which are separated by catalytically relevant interdomain linkers that show organization upon tRNA binding.¹⁶ The analogue of TrmD in archaea and eukaryotes, TrmS, is structurally distinct with a differing SAM binding mode.¹⁷ This reduces the chance of an inhibitor of *Mab* TrmD binding off-site in the human host, making this essential enzyme an attractive target for drug development.

The attractiveness of TrmD as a target is reflected in the recent application of a high-throughput screen against TrmD from *P. aeruginosa* to identify low-micromolar inhibitors.¹⁸ However, there are currently on-going efforts to validate the in vivo mechanism of these compounds before they are further developed as antibiotics. Structure-driven fragment-based methods provide an alternative methodology for the efficient design of potent inhibitors from low-molecular weight starting points and are now firmly established in both academia and industry.¹⁹ A fragment-based approach was used in a prior study against *Haemophilus influenzae* TrmD to develop selective inhibitors that ordered the interdomain linker in a similar manner to tRNA.²⁰ Disappointingly, in general, these compounds only displayed weak activity when screened against a range of Gram-positive and Gram-negative pathogens, including efflux mutant strains of *Escherichia coli* and *H. influenzae*. In this work, a fragment-based approach was employed to design potent inhibitors against *Mab* TrmD that show growth inhibition across a range of pathogenic mycobacteria.

RESULTS AND DISCUSSION

A fragment library of 960 fragments was screened against TrmD using differential scanning fluorimetry (DSF) as a primary

screen. This resulted in 53 hits with a thermal shift cut-off value of 3 standard deviations from the negative control. These hits were then carried forward for soaking experiments using X-ray crystallography. Of these hits, density was observed for 27 fragments, all of which were shown to bind at the SAM binding pocket of *Mab* TrmD. The remaining 26 fragments did not show any electron density.¹² This work herein describes the use of fragment-growing and merging strategies on fragment hits to develop novel compounds to inhibit *Mab* TrmD. Using the fragment-merging strategy, compounds have been developed that afford up to a 4-order of magnitude improvement in affinity against *Mab* TrmD, combined with inhibition of *Mab* growth in vitro and in a human macrophage infection model. A number of these key compounds display potent inhibition of *Mtb* growth in vitro, while one of the lead molecules also exhibits growth inhibition of intracellular *Mycobacterium leprae*.¹²

Fragment-Growing Strategy. The SAM co-factor has been shown by X-ray crystallography to bind to *Mab* TrmD simultaneously in the two symmetry-related active sites, with the adenine ring “anchoring” the molecule in place through hydrogen bonds to the backbone amides of residues Ile133, Gly134, Tyr136, and Leu138 (Figure 1a).¹² This is formed from the loop of Val131 to Leu138, bordered behind and above by Pro83 and Pro85, and below by Ile133, Tyr136, Leu138, and Ala144, encompassing the “adenine binding pocket”. Fragment hit **1** (K_d 89 μ M, LE 0.55, Table 1) was observed by X-ray crystallography to occupy the adenine binding pocket, with the pyrazole ring hydrogen bonding to the backbone amides of Gly134 and Ile133, and the carbonyl oxygen engaging the backbone amide of Leu138 (Figure 1b). This highly ligand-efficient fragment was chosen as a starting point for a fragment-growing strategy (Table 1). DSF screening was used as a first line screen with the elaborated compounds as a guide to prioritize compounds for isothermal titration calorimetry (ITC). The ester group of **1** was shown to be resistant to replacement, with the amide analogue **2** giving a thermal shift below +0.5 °C at 5

Table 1. Change in the Melting Temperatures (ΔT_m), Affinities (K_d), and Ligand Efficiencies (LE) of Fragment Hit 1 and Compounds 2–7

compound	ΔT_m^a (°C)	R	K_d (μM)	LE ^b
1 (X = O)	+0.4 ^c		89 ± 4	0.55
2 (X = NH)	ND ^d		ND	
3	+3.1	H	33 ± 2	0.41
4	+0.4	4-NO ₂	ND	
5	+0.9	4-CO ₂ Me	ND	
6	+2.8	3-CN	30 ± 1	0.36
7	+3.5	3-OMe	14 ± 1	0.39

^a100 μM ligand and 10 μM *Mab* TrmD. ^bkcal mol⁻¹ per heavy atom. ^cDetermined to be +4.0 °C with 5 mM ligand and 10 μM *Mab* TrmD. ^dDetermined to be +0.4 °C with 5 mM ligand and 10 μM *Mab* TrmD.

mM (+4.0 °C for 1) by DSF. From the X-ray crystal structure, the ethyl chain of 1 extends into the region occupied by the ribose portion of SAM, the “ribose binding pocket” (Figure 1a,b). This was used as a vector for a fragment-growing strategy. The phenyl ring introduced in 3 (K_d 33 μM , LE 0.41) was shown by X-ray crystallography to occupy the ribose-binding pocket (Figure S1a). This induced a movement in Tyr111 (2.5–5.1 Å at C- α depending on the active site), similar to that shown in the SAM-bound *Mab* TrmD X-ray crystal structure. From the synthesized analogues of 3 with varying substituents, 7 (K_d 14 μM , LE 0.39) demonstrated a ligand-efficient improvement in binding affinity. The X-ray crystal structures of 7- and 3-bound *Mab* TrmD both showed evidence of a second ligand molecule in the active site bound to the backbone amide nitrogen of Glu180 through its carbonyl oxygen (Figures 1c and S1a).

Compound 7 was used as the basis for further derivatives (Table 2), initially from the use of the 3-methoxy group as a vector for growth (see Figure S1). The use of aromatic rings in 9 (ΔT_m +2.5 °C) and 11 (ΔT_m +3.0 °C), an ester group in 8 (K_d 10 μM , LE 0.32) or chain extension in 10 (K_d 11 μM , LE 0.38) did not result in either a significant improvement in binding affinity or, when this was not determinable by ITC, an increase in thermal shift. The observation of a second ligand molecule for 7 in the active site was exploited for a fragment linking approach, with the attachment of a molecule of 1 to the scaffold of 7 through a propargyl linker in 12 (K_d 4.6 μM , LE 0.24); however, while an improved binding affinity was achieved, the ligand efficiency was adversely affected. The 5-position of the phenyl ring of 7 was also utilized as a vector for growth for the insertion of ring systems into the volume bordered by residues Glu112, Val137, Arg154, and Glu180. However, while the added pyrrolidinyl and pyridyl groups were tolerated in 13 (K_d 10 μM , LE 0.31) and 14 (K_d 6.7 μM , LE 0.31), a significant improvement in affinity was again not achieved, including with the addition of a methylene linker in 15 (K_d 12 μM , LE 0.28). Protein X-ray crystallography showed that the added groups in 8 and 14 did reach the desired regions of the active site in *Mab* TrmD (Figure S1b,c); however, attempts to improve the affinity using the stated strategies proved challenging. The lack of increase in affinity and the liability of the ester functional group

Table 2. Change in the Melting Temperatures (ΔT_m), Affinities (K_d), and Ligand Efficiencies (LE) of Compounds 8–15

Compound	ΔT_m^a (°C)	R ¹	R ²	K_d (μM)	LE ^b
8	+2.6	CO ₂ Me	H	10 ± 1	0.32
9	+2.5		H	ND	-
10	+3.1	Me	H	11 ± 1	0.38
11	+3.0		H	ND ^c	-
12	+9.6	H		4.6 ± 0.7	0.24
13	+3.0	H		10 ± 2	0.31
14	+3.8	H		6.7 ± 0.6	0.31
15	+3.0	H		12 ± 1	0.28

^a100 μM ligand and 10 μM *Mab* TrmD. ^bkcal mol⁻¹ per heavy atom. ^cNot determined due to solubility.

in these compounds pointed to the need to develop an alternative strategy to target *Mab* TrmD.

Fragment-Merging Strategy. In a similar way to compound 1 (K_d 89 μM , LE 0.55, Table 2), the aminopyrazole ring system of fragment hit 16 (K_d 170 μM , LE 0.37) occupied the adenine binding pocket, with the pyrazole ring hydrogen bonding to the backbone amides of Tyr136 and Leu138 and the amino group engaging Gly134 and the alcohol side chain of Ser132 (Figure 2a). In contrast, the 4-methoxyphenyl ring of 16 extended into the ribose binding pocket. The methoxy group showed no direct interactions with the surrounding residues; however, the corresponding phenyl (17) and 4-tolyl (18) analogues lacking the methoxy group afforded relatively low ΔT_m values (1.4–1.5 °C). The methoxy group of 16 was also shown to possess a preference for the 4-position of the phenyl ring, with the 3-methoxyphenyl analogue 19 providing a negative thermal shift (Table 3). The ribose binding pocket was shown to be occupied by the indole ring of fragment hit 20 (K_d 260 μM , LE 0.41), where the indole nitrogen indirectly interacts with the backbone carbonyl of Leu138 through a water molecule. The 6-boronic acid group of 20 partially extends into the adenine binding pocket, engaging the backbone amides of residues Tyr136 and Leu138 through hydrogen bonds, as well as two water molecules that occupy the remaining space in the pocket, interacting with the backbone amides of Val131, Ile133, and Gly134 in addition to the side chain of Ser132 (Figure 2b). The isosteric replacement of the boronic acid group with a carboxylic acid, as shown in fragment 21, was shown to not be tolerated, with no ΔT_m observed. Further, examination of the structure with 5-boronic acid isomer 22 bound using X-ray crystallography showed the indole ring “flipping” to maintain the

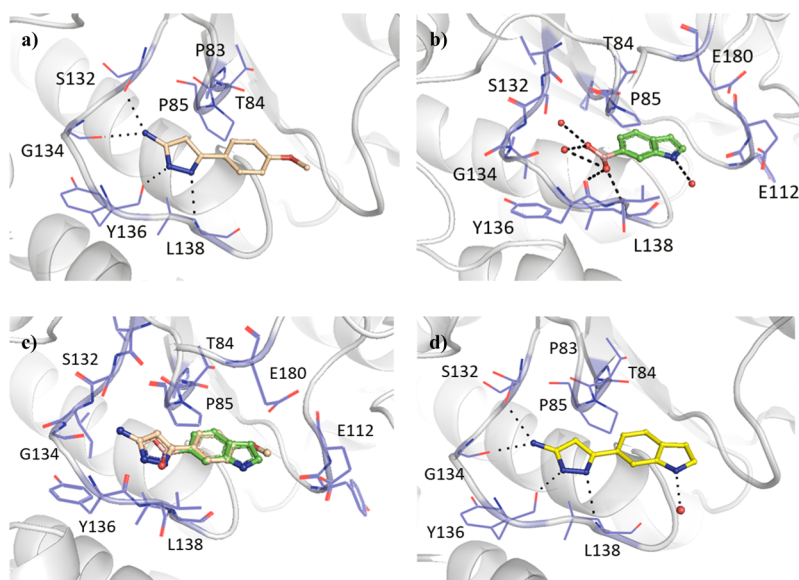


Figure 2. X-ray crystal structures of *Mab* TrmD in complex with (a) **16** (PDB code 6QOT), (b) **20** (PDB code 6QOU), (c) **16** and **20** (overlay of PDB code 6QOT and PDB code 6QOU), and (d) **23** (PDB code 6QQS), illustrating one of the active sites.¹²

Table 3. Change in the Melting Temperatures (ΔT_m), Affinities (K_d), and Ligand Efficiencies (LE) of Fragment Hits **16** and **20**, Their Structural Analogues **17–19** and **21–22**, and Compound **23**

16 - 19		20 - 22		23	
compound	R ¹	R ²	ΔT_m^a (°C)	K_d (μ M)	LE ^b
16 ^c	4-OMe		+3.0	170 \pm 10	0.37
17	H		+1.5	ND	
18	4-Me		+1.4	ND	
19	3-OMe		-0.5	ND	
20 ^c		6-B(OH) ₂	+4.0	260 \pm 20	0.41
21		6-CO ₂ H	-0.6	ND	
22		5-B(OH) ₂	+1.3	ND	
23 ^d			+4.8 ^e	110 \pm 10	0.36

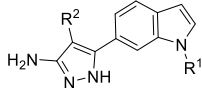
^a5 mM ligand and 10 μ M *Mab* TrmD. ^bkcal mol⁻¹ per heavy atom. ^c ΔT_m , K_d and LE previously reported.¹² ^d K_d and LE previously reported.¹² ^eDetermined to be +1.1 °C with 100 μ M ligand and 10 μ M *Mab* TrmD.

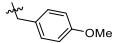
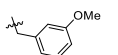
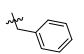
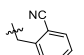
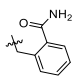
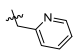
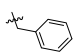
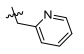
hydrogen bonding interactions of the boronic acid, with the indole nitrogen interacting with an extensive hydrogen-bonded water network in the rear of the active site (Figure S2a). Even though the boronic acid of **22** was shown to form the same hydrogen-bonding water network in the adenine binding pocket as **20**, it gave a lower ΔT_m (Table 3). The overlap of the respective 4-methoxyphenyl and indole ring systems of **16** and **20** (Figure 2c), and their spanning of the adenine and ribose binding pockets, offers the possibility of a fragment-merging strategy. This was explored successfully with **23** (K_d 110 μ M, LE 0.36), providing a new aminopyrazole-indole scaffold with both improved affinity and prospects for further elaboration relative to the parent fragments (Figure 2d). Compound **23** was shown by X-ray crystallography to maintain the hydrogen-bonding interactions of the original fragment **16**, which remained unaffected throughout all subsequent additions to the scaffold,

with the indole nitrogen providing a vector for elaboration that the fragment hit **16** lacked.

Elaboration of Compound 23. Elaboration of **23** was initially carried out from the indole nitrogen with the introduction of a 4-methoxybenzyl group in **24a** (K_d 59 μ M, LE 0.24) (Table 4). While the gain in affinity was less than desired, the added group reached the portion of the active site occupied by the methionine moiety of SAM defined by Pro85, Glu112, Val137, Arg154, and Glu180 (Figure 3a). The synthesis of the 3-methoxybenzyl **24b** (K_d 13 μ M, LE 0.28) and benzyl **24c** (K_d 19 μ M, LE 0.29) derivatives demonstrated improved affinities (GE 0.14 and 0.15, respectively). While the 2-benzamide **24e** gave a lower ΔT_m of +1.4 °C, further improvements in affinity were realized relative to **24c** with the synthesis of the 2-cyanobenzyl **24d** (K_d 12 μ M, LE 0.28) and 2-picoyl **24f** (K_d 12 μ M, LE 0.30) analogues. Attention was also focused on elaboration from the 4-position of the pyrazole ring of **23**. This vector was shown by X-ray crystallography to face a narrow and elongated pocket formed by Pro83, Thr84, Val131, Ser132, Ile133, and Ala144 (Figure 2d). The addition of a nitrile group in **25** (K_d 5.0 μ M, LE 0.43) afforded a jump in affinity from **23** (K_d 110 μ M, LE 0.36), with the added functionality highly group efficient (GE 0.91). An X-ray crystal structure of **25** bound to TrmD showed that the nitrile extended into the pocket, engaging the backbone amides of Thr84 and Ile133, with no major changes in the ligand binding orientation or conformation of neighboring residues (Figure 3e). The nitrile was subsequently incorporated into **24f** to afford **26f** (K_d 0.50 μ M, LE 0.36), with the added nitrile functional group affording a similar jump in affinity as in **25** (GE 0.95 and 0.91 respectively).

Following the development of **26f**, the corresponding 3-pyridyl isomer **26g** (K_d 0.18 μ M, LE 0.38, Table 5) afforded a greater than 2-fold improvement in binding affinity without additional interactions being observed in the X-ray crystal structure of ligand-bound *Mab* TrmD (Figures 3f and 4a). The late stage functionalization of **26g** through addition of a chlorine atom on the 3-position of its indole ring in **27g** (K_d 8.5 μ M, LE 0.28) was not tolerated (Table 5). While this modification of **26g** did not result in a significant shift in the indole ring, one of the ordered water molecules in the rear of the active site bound

Table 4. Change in the Melting Temperatures (ΔT_m), Affinities (K_d), and Efficiency Metrics of Compounds **24a–f**, **25**, **26c**, and **26f**


Compound	R ¹	R ²	ΔT_m^a (°C)	K_d (μ M)	LE ^b	GE ^b (R ¹)	GE ^b (R ²)
24a		H	+3.4	59 ± 17	0.24	0.04	-
24b		H	+4.6	13 ± 2	0.28	0.14	-
24c		H	+3.4	19 ± 1	0.29	0.15	-
24d		H	+4.4	12 ± 2	0.28	0.15	-
24e		H	+1.4	ND	-	-	-
24f^c		H	+3.1	12 ± 1	0.30	0.18	-
25	H	CN	+4.4	5.0 ± 2.1	0.43	-	0.91
26c		CN	+10.1	ND ^d	-	-	-
26f^c		CN	+8.3	0.50 ± 0.14	0.36	0.20	0.95

^a100 μ M ligand and 10 μ M *Mab* TrmD. ^bkcal mol⁻¹ per heavy atom. ^c K_d and LE previously reported.¹² ^dNot determined due to solubility.

to Pro83 was displaced (Figure 4b). 2-Hydroxypyridyl/pyridone derivatives of **26g**, **26j** (K_d 3.2 μ M, LE 0.30), and **26k** (K_d 1.3 μ M, LE 0.32) were synthesized to engage neighboring residues Arg154 and Glu180, respectively, through the added oxygen atoms. While the X-ray crystal structure of *Mab* TrmD with **26j** bound did show evidence of a hydrogen bond between the added oxygen atom of the ligand and Arg154 (Figure 4c), neither derivative possessed an improved binding affinity. In contrast, the exploration of the alternative 4-pyridyl isomer **26l** (K_d 0.12 μ M, LE 0.39) resulted in a 4-fold decrease of K_d value relative to **26f**, with the nitrogen atom of its pyridyl ring lying 2.9 Å from the carboxylate group of Glu180 (Figure 4d).

Modification of the pyridyl ring of **26l** to the corresponding 4-quinolyl ring system in **26m** afforded a significant thermal shift (ΔT_m +10.3 °C at 100 μ M), suggesting that the bicyclic ring was tolerated (Table 5). However, this modification adversely affected solubility, precluding the determination of binding affinity by ITC at the desired concentrations. The replacement of the pyridyl ring with more soluble saturated alternatives resulted in the development of racemic compounds *N*-methyl piperidin-2-yl **26n** (K_d 0.59 μ M, LE 0.34) and *N*-methyl piperidin-3-yl **26o** (K_d 0.36 μ M, LE 0.35), whose ITC isotherms could be fitted by a one-site binding model (Figures S7d and S8a). However, racemic mixtures can afford deceptively simple isotherms under certain circumstances, such as when the enthalpies of binding of the individual enantiomers are equivalent, with the curve mimicking the K_d of the weaker component.²¹ Hence, a reverse ITC titration was also performed for **26o**. This afforded a simple curve that could be fitted by similar parameters to the forward titration (Figure S8b), implying that the enantiomers of **26o** are equipotent. The X-ray crystal structure of **26n** showed that the nitrogen atom of its piperidinyl ring interacts with the backbone carbonyl of Tyr111

(Figure S2c), while that of **26o** formed electrostatic interactions with either of Glu112 or Glu180 depending on the active site (Figure 4e,f).

The targeting of Glu112 and Glu180 through electrostatic interactions with saturated heterocyclic ring systems was continued, with the pyridyl ring of **26f** providing a good starting point for the presentation of amines at the top of the active site (Table 6). The implementation of a similar strategy against *H. influenzae* TrmD with engagement of the catalytic residue Asp169 resulted in improved inhibition and the ordering of the interdomain linker.²⁰ The addition of a pyrrolidinyl ring through a methylene linker to **26f** in **28** (K_d 92 nM, LE 0.32) showed that the strategy was applicable to this lead series. Modification of the scaffold through replacement of the pyridyl ring of **28** with a phenyl ring in **29a** (K_d 27 nM, LE 0.34) was beneficial to the binding affinity, in contrast to the difference in affinities between the phenyl and pyridyl derivatives **24c** (K_d 19 μ M, LE 0.29) and **24f** (K_d 12 μ M, LE 0.30). The X-ray crystal structure of *Mab* TrmD in complex with **29a** showed the pyrrolidinyl ring occupying the binding sites in two conformations, thereby interacting with the carboxylates of either Glu112 or Glu180, while Asp169 and the rest of the interdomain linker remained unstructured (Figure 5a,b). Replacement of the nitrile group on the 4-position of the pyrazole ring of **29a** was also explored through the methyl-substituted alternative **30a** (K_d 2.0 μ M, LE 0.27), which showed a higher binding affinity than the unsubstituted derivative **31a** (K_d 0.49 μ M, LE 0.31). Derivatives of **29a** with alternative substituents in place of its pyrrolidinyl ring were trialed, including **29b** (K_d 70 nM, LE 0.31) whose piperidinyl ring was shown to interact with Glu112 in preference to Glu180 (Figure 5c). The use of a morpholinyl ring resulted in a significant attenuation of binding affinity in **29c** (K_d 0.19 μ M, LE 0.30), possibly because of the impact of reduced basicity of

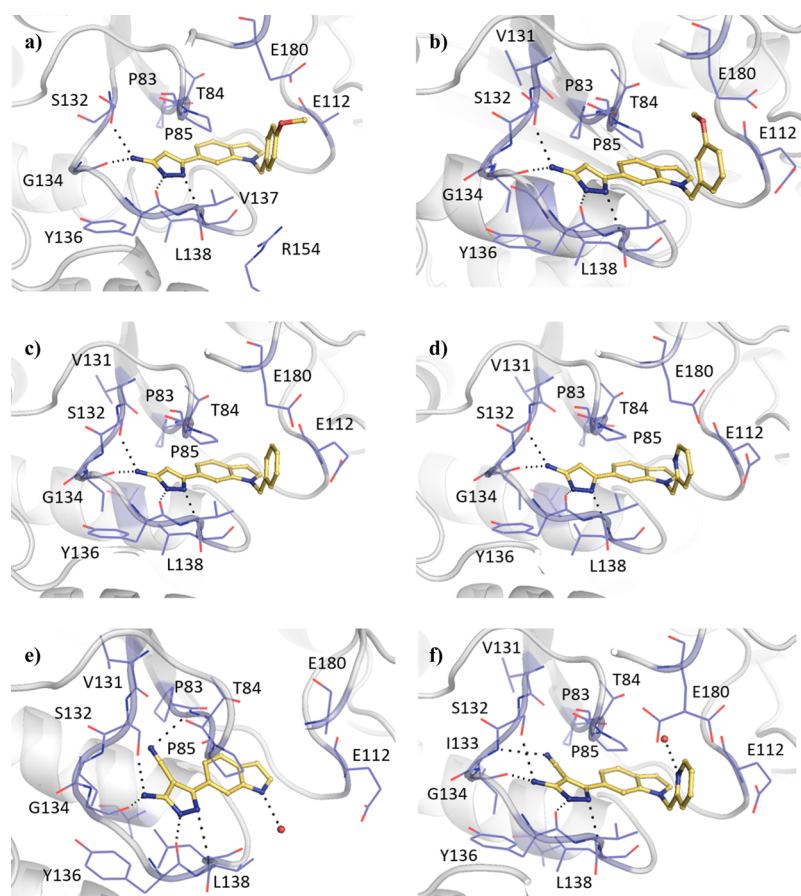


Figure 3. X-ray crystal structures of *Mab* TrmD in complex with (a) **24a** (PDB code 6QQT), (b) **24b** (PDB code 6QRC), (c) **24c** (PDB code 6QQW), (d) **24f** (PDB code 6QQX),¹² (e) **25** (PDB code 6QQU), and (f) **26f** (PDB code 6QQY),¹² illustrating one of the active sites.

Table 5. Change in the Melting Temperatures (ΔT_m), Affinities (K_d), and Efficiency Metrics of Compounds **26g**, **26j**–**o**, and **27g**

Compound	R ¹	R ²	ΔT_m^a (°C)	K_d (μ M)	LE ^b	GE ^b (R ¹)
26g		H	+10.5	0.18 ± 0.06	0.38	0.28
26j		H	+5.5	3.2 ± 0.3	0.30	0.03
26k		H	+8.3	1.3 ± 0.1	0.32	0.10
26l		H	+11.5	0.12 ± 0.02	0.39	0.31
26m		H	+10.3	ND ^c	-	-
26n		H	+8.8	0.59 ± 0.23	0.34	0.16
26o		H	+10.9	0.36 ± 0.05	0.35	0.20
27g		Cl	+5.8	8.5 ± 1.0	0.28	-

^a100 μ M ligand and 10 μ M *Mab* TrmD. ^bkcal mol⁻¹ per heavy atom. ^cNot determined due to solubility.

the morpholinyl nitrogen on its interactions with Glu112 and Glu180. Protein X-ray crystallography showed that compound **29c** adopted a similar binding pose as **29b**, but with the morpholinyl ring rotated and orienting its oxygen atom toward Pro57 (Figure 5d). In contrast to **29c**, the *N*-methyl piperazinyl ring of **29d** (K_d 73 nM, LE 0.30) was oriented away from Glu112 with its methyl group extending further into the pocket defined by the loop from Ala176 to Glu180 (Figure 5e). The methyl substituent on the piperazinyl ring of **29d** was expanded to an isopropyl group in **29e** (K_d 0.10 μ M, LE 0.28), whose electron density maps suggest two alternative binding poses with the isopropyl group oriented toward either Glu112 or the loop from Ala176 to Glu180 at the top of the active site (Figure 5f).

Native Mass Spectrometry. Native mass spectrometry (native MS) was used to investigate the structure and interactions of *Mab* TrmD. The protein alone presented as the dimer with an observed mass of 53 187 Da, centered around the 15+ charge state (Figure 6). The observed mass is slightly higher than the theoretical mass of 52 520 Da because of the presence of solvent and buffer molecules that remain weakly bound to the protein under the soft ionization conditions employed.²² In the presence of 5% dimethylsulfoxide (DMSO), the native mass spectrum of *Mab* TrmD shifted to a lower charge state distribution (Figure 6). This is consistent with previous studies on the effect of DMSO on protein charging in electrospray ionization (ESI).^{23,24}

Native MS was used to study the interaction between the small molecules and *Mab* TrmD. A titration experiment performed with **24c** revealed increasing occupancy of the

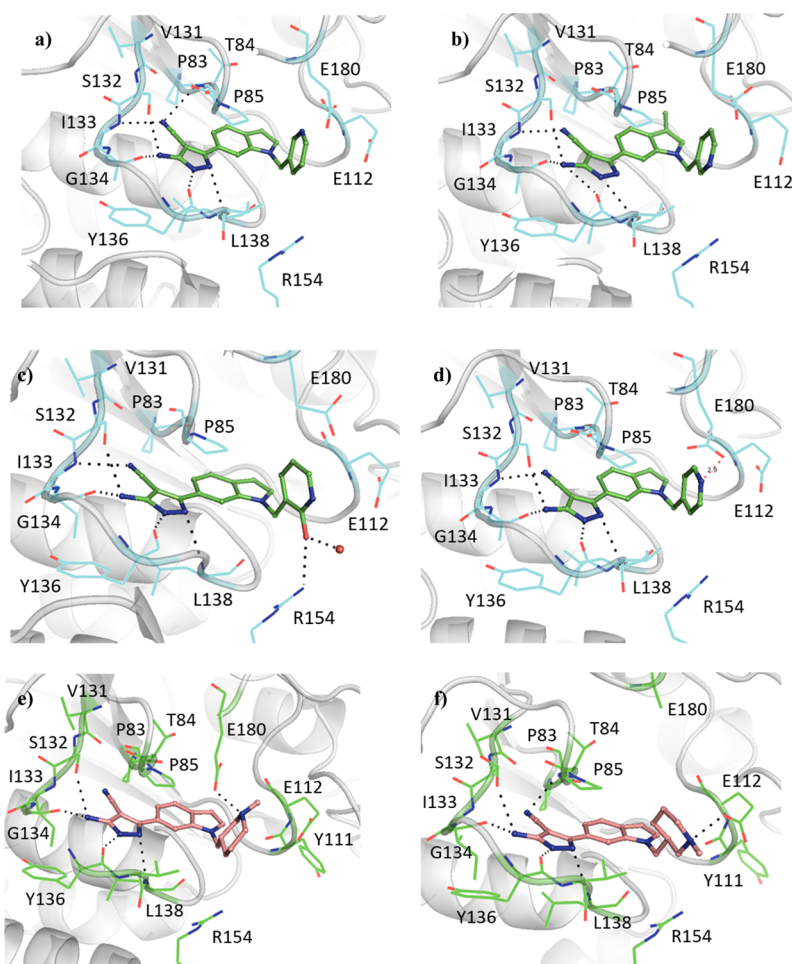


Figure 4. X-ray crystal structures of *Mab* TrmD in complex with (a) **26g** (PDB code 6QQZ), (b) **27g** (PDB code 6QR1), (c) **26j** (PDB code 6QR2), and (d) **26l** (PDB code 6QR0), illustrating one of the active sites, and *Mab* TrmD in complex with **26o** (PDB code 6QR3), illustrating active sites 1 (e) and 2 (f).

Table 6. Change in the Melting Temperatures (ΔT_m), Affinities (K_d), and Efficiency Metrics of Compounds **28, **29a–e**, **30a**, and **31a–b****

Compound	X	R ¹	R ²	ΔT_m^a (°C)	K_d (nM)	LE ^b	GE ^b (CH ₂ R ¹)
28^c	N		CN	+12.0	92 ± 18	0.32	0.17
29a^c	CH		CN	+12.9	27 ± 4	0.34	-
29b	CH		CN	+12.6	70 ± 29	0.31	-
29c	CH		CN	+12.6	190 ± 23	0.30	-
29d^c	CH		CN	+12.0	73 ± 30	0.30	-
29e	CH		CN	+11.9	100 ± 24	0.28	-
30a	CH		Me	+6.1	2000 ± 310	0.27	-
31a^c	CH		H	+7.0	490 ± 210	0.31	0.36
31b	CH		H	+7.2	710 ± 90	0.29	0.28

^a100 μ M ligand and 10 μ M *Mab* TrmD. ^bkcal mol⁻¹ per heavy atom. ^c K_d and LE previously reported.¹²

protein as the concentration of the ligand was increased (Figure 6). At 20 μ M of *Mab* TrmD and 12.5 μ M of **24c** (with 5% DMSO), a single molecule of the ligand could be observed to bind to the 13+ charge state of the protein, although the majority of that charge state remained unbound. At 25 μ M of **24c**, both singly and doubly bound *Mab* TrmD could be detected at the 13+ charge state. The proportion of doubly bound *Mab* TrmD increased at 50 μ M of **24c**, while at 100 μ M, the 13+ charge state of the protein was entirely doubly bound. A similar trend could be observed for the 14+ charge state, except that the degree of occupancy of the protein was lower at each concentration of **24c** due to the greater Coulombic repulsion experienced by the protein-ligand complexes at 14+ compared to at 13+. The lack of triply bound *Mab* TrmD observed even at excess concentrations of **24c** suggests that little, if any, of the small molecule bound non-specifically to the protein dimer.

Compounds **26c** and **29a** were also screened against *Mab* TrmD using native MS at a ligand concentration of 100 μ M (Figure 6). Interestingly, despite its tight binding affinity for *Mab* TrmD as measured by ITC, complexes formed with **29a** showed low gas-phase stabilities in native MS. Dissociation of **29a** from *Mab* TrmD led to a shift in the charge state distribution of the protein to lower charge states, which was confirmed for individual precursor charge states by MS/MS (data not shown). This could be rationalized by the dissociation of positively charged **29a** molecules from *Mab* TrmD, leading to a reduction

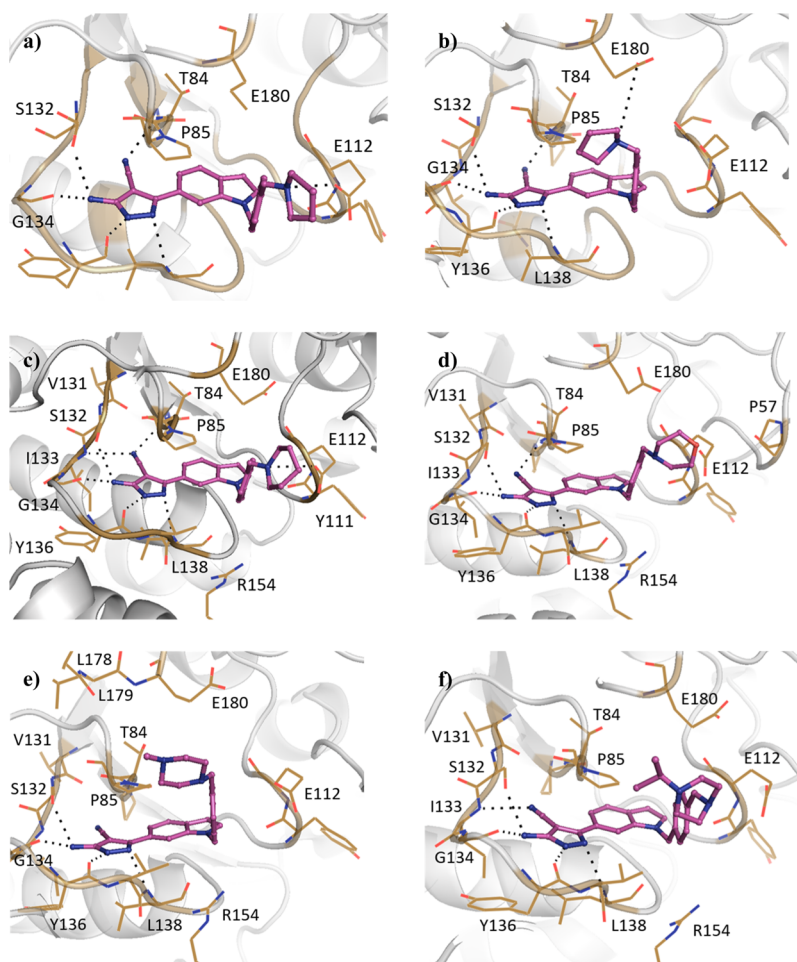


Figure 5. X-ray crystal structures of *Mab* TrmD in complex with **29a** (PDB code 6QR6),¹² illustrating active sites 1 (a) and 2 (b), and *Mab* TrmD in complex with (c) **29b** (PDB code 6QR7), (d) **29c** (PDB code 6QR9), (e) **29d** (PDB code 6QR8),¹² and (f) **29e** (PDB code 6QRD), illustrating one of the active sites.

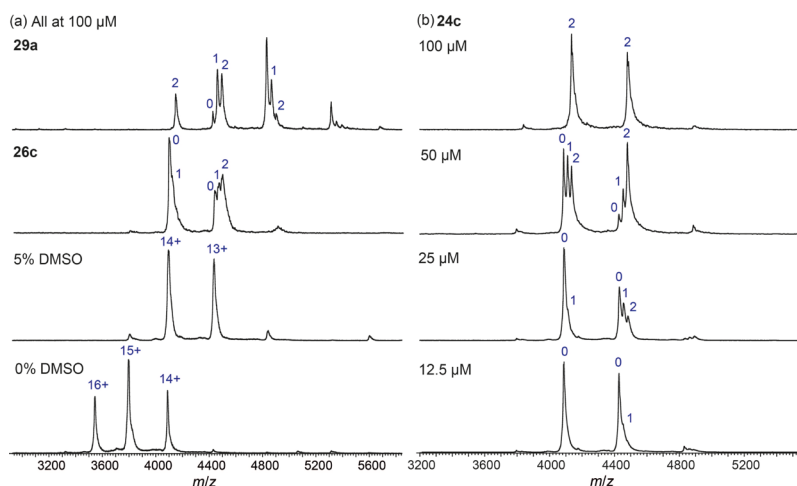
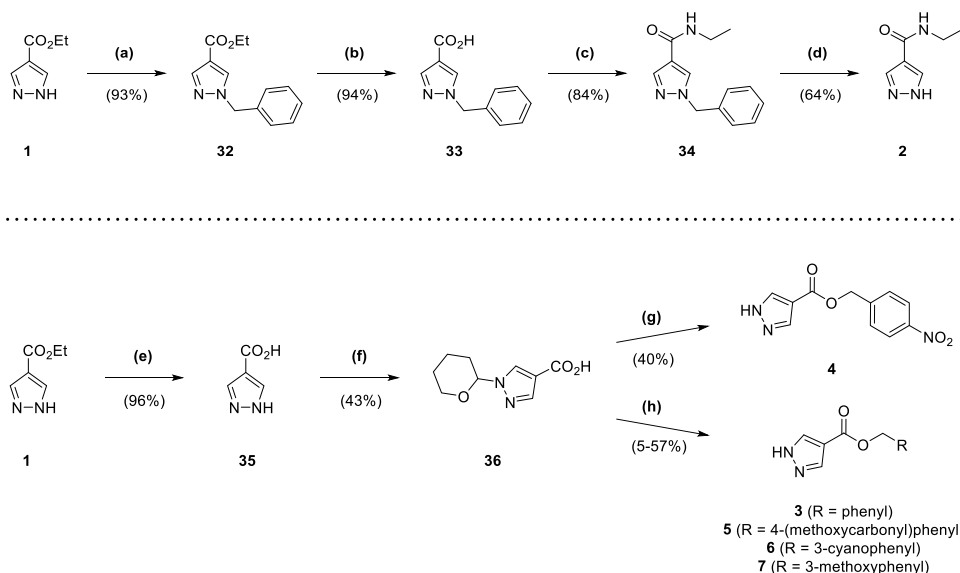


Figure 6. Native mass spectrometry of *Mab* TrmD with compounds **24c**, **26c**, and **29a**. Experiments with ligands contain 5% DMSO.

of the overall positive charge of the protein. In contrast, **24c** and **26c**, being potentially less cationic than **29a**, did not exhibit this charge reduction behavior. Overall, the native MS data confirm the direct binding of the ligands to *Mab* TrmD and suggest that the interaction is specific, with each *Mab* TrmD dimer binding to two molecules of the ligand.

Synthetic Chemistry. Synthesis of compound **2** (Scheme 1) began with addition of a benzyl protecting group to fragment hit **1** through heating at reflux with benzyl bromide in acetone (93% yield), followed by alkaline hydrolysis of the ester group of **32** to a carboxylic acid (94% yield). Acid **33** was converted by the action of 1-ethyl-3-(3-dimethylaminopropyl)carbodiimide (EDC) to the amide **34** (84% yield) and then debenzylated to **2**

Scheme 1. Synthesis of Compounds 2–7^a

^aReagents and conditions: (a) BnBr, K₂CO₃, acetone, reflux, 7 h; (b) NaOH, THF, H₂O, 70 °C, 150 min; (c) EtNH₂·HCl, DIPEA, DMAP, EDC·HCl, DCM, 15 h; (d) Pd/C (10 wt % loading), formic acid, ^tBuOH, 50 °C, 2 h; (e) NaOH, H₂O, reflux, 2 h; (f) 3,4-dihydro-2H-pyran, TsOH·H₂O, EtOAc, DMF, overnight; (g) (i) 4-nitrobenzyl alcohol, DIPEA, DMAP, EDC·HCl, DCM, overnight (ii) TFA, 5 min; (h) (i) RCH₂Br, DIPEA, DMF, 90 min to 2 h (ii) TFA, 10–12 min.

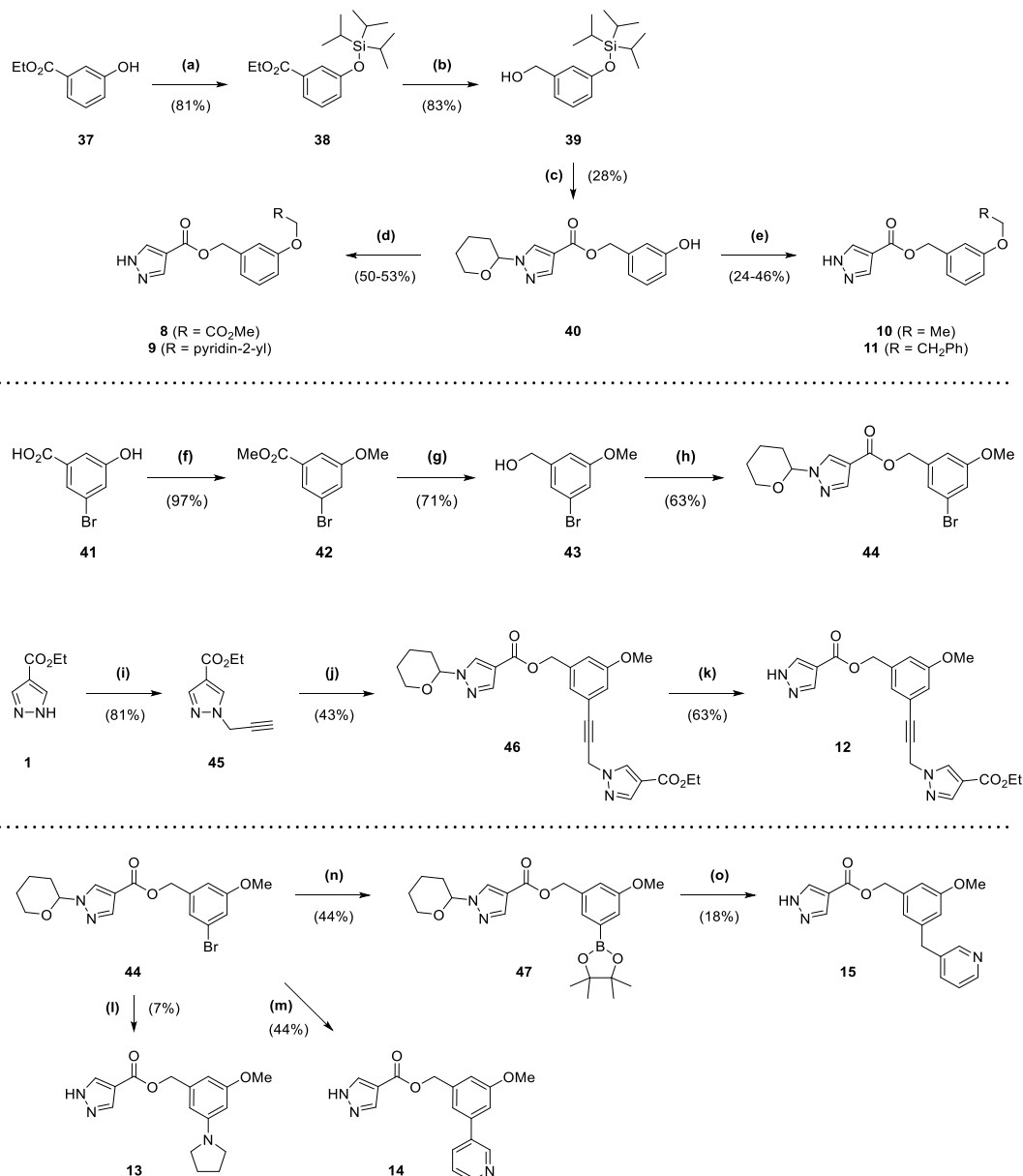
through transfer hydrogenation with palladium on carbon, formic acid, and *tert*-butanol (64% yield). The production of esters 3–7 (Scheme 1) started with hydrolysis of 1 to the corresponding carboxylic acid 35 (96% yield), whose pyrazole was protected with a tetrahydropyran ring through treatment with 3,4-dihydro-2H-pyran under acidic conditions to give 36 (43% yield). Carboxylic acid 36 was used to synthesize the final ester compounds 3–7 by two alternative two step protocols, involving either initial treatment with a benzyl halide and base in dimethylformamide (DMF) or EDC-mediated ester coupling with a benzyl alcohol. Both protocols ended with removal of the tetrahydropyran protecting group by trifluoroacetic acid (TFA; 5–57% yield overall).

The routes for synthesis of compounds 8–11 (Scheme 2) involved protection of phenol 37 with a triisopropylsilyl protecting group (81% yield), followed by reduction of the ester group of 38 to the corresponding alcohol 39 using lithium aluminium hydride (83% yield). Alcohol 39 was put through an EDC-mediated ester coupling reaction with 36, with the silyl protecting group removed using tetra-*n*-butylammonium fluoride (TBAF; 28% yield overall). Phenol 40 was treated with an alkyl bromide and base in DMF, and then the tetrahydropyran-protecting group was removed with TFA to afford 8 and 9 (50–53% yield overall). In contrast, 10 and 11 were synthesized from 40 through initial coupling with an alcohol under Mitsunobu conditions with triphenylphosphine and diisopropyl azodicarboxylate, followed by treatment with TFA (24–46% yield overall). Compounds 12–15 all utilized bromoarene 44 in their respective syntheses (Scheme 2), itself synthesized by a sequence involving methyl iodide alkylation of 41 (97% yield), followed by lithium aluminium hydride reduction of ester 42 to alcohol 43 (71% yield) that was coupled with 36 using EDC (63% yield). The Sonogashira cross-coupling of 44 with alkyne 45, itself produced by treatment of fragment hit 1 with propargyl bromide in a suspension of potassium carbonate and DMF (81% yield), afforded 46 (43% yield). TFA-mediated deprotection of 46 provided 12 (63%

yield). 13 was synthesized by Buchwald–Hartwig amination of 44 with pyrrolidine, followed by TFA deprotection (7% yield overall). In contrast, 14 was produced through a Suzuki–Miyaura cross-coupling reaction of 44 with 3-(bromomethyl)pyridine, followed by TFA deprotection (44% yield overall). For 15, 44 was converted to the corresponding pinacol boronic ester 47 by a Miyaura-borylation with bis(pinacolato)diboron (44% yield), which was then cross-coupled with 3-(bromomethyl)pyridine in a Suzuki–Miyaura reaction and deprotected with TFA (18% yield overall).

The synthetic route for the 5-aminopyrazole analogue 19 (Scheme 3) began with nucleophilic attack of ester 48 by a nitrile anion, generated from *n*-butyllithium and acetonitrile. This resulted in the corresponding β -ketonitrile 49 (99% yield), which was heated at reflux with hydrazine in ethanol to form 19 (73% yield).²⁵ The synthesis of 23 (Scheme 3) was similar to 19, using indole 50 as the starting point, which was protected with a *tert*-butyldimethylsilyl group to form 51 (59% yield). After synthesis of the corresponding β -ketonitrile, deprotection was accomplished by TBAF without prior purification affording 52 (99% yield overall), which was heated at reflux with hydrazine in ethanol (59% yield). The deprotected β -ketonitrile 52 was also utilized in the synthesis of 25 (Scheme 3), with its activated methylene group treated with trichloroacetonitrile and sodium acetate.²⁶ The resultant functionalized compound 53 was purified (87% yield) before heating at reflux with hydrazine in ethanol to afford 25 (24% yield).

Synthesis of compounds 24a–c and 24f (Scheme 3) utilized formation of β -ketonitriles 55a–c and 55f from the corresponding methyl esters 54a–c and 54f (84–99% yield) and subsequent reaction with hydrazine (31–62% yield). Unlike 23, the indole nitrogen was protected by the benzyl or picolyl groups. In the cases of 54a–d and 54f, these were added to indole 50 by heating at reflux with caesium carbonate and benzyl or picolyl halides in acetonitrile (80–93% yield). Because of the production of significant amounts of side products in the synthesis of the corresponding β -ketonitrile from 54d, the

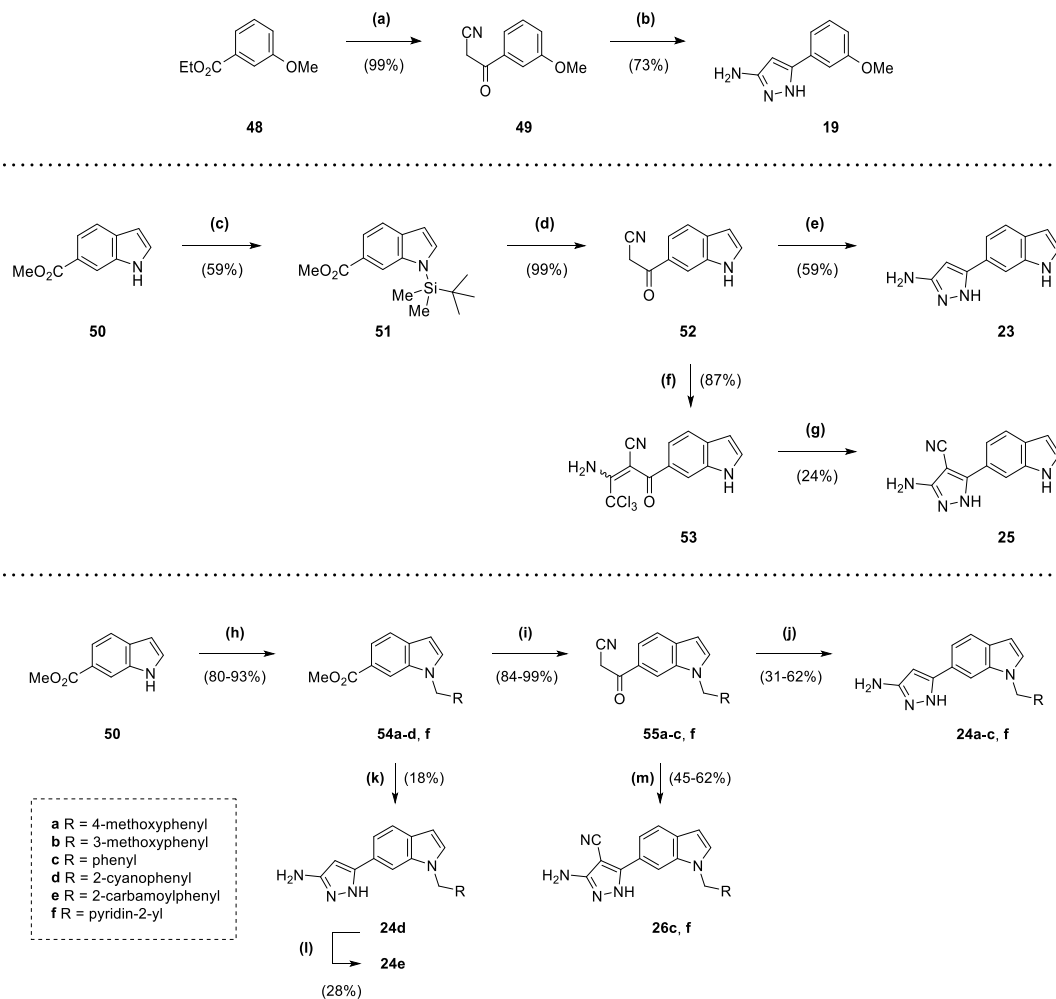
Scheme 2. Synthesis of Compounds 8–15^a

^aReagents and conditions: (a) TIPSCl, imidazole, DMF, 2 h; (b) LiAlH₄ (2.4 M in THF), Et₂O, 0 °C to rt, 3 h; (c) (i) **36**, DIPEA, DMAP, EDC·HCl, DCM, overnight (ii) TBAF (1 M in THF), 10 min; (d) (i) Cs₂CO₃, RCH₂Br (·HBr), DMF, 2 h (ii) TFA, 15 min; (e) (i) PPh₃, RCH₂OH, DIAD, THF, 1 h to overnight (ii) TFA, 15 min; (f) MeI, K₂CO₃, DMF, 3 d; (g) LiAlH₄ (2.4 M in THF), Et₂O, 0 °C to rt, overnight; (h) **36**, DIPEA, DMAP, EDC·HCl, DCM, overnight; (i) propargyl bromide (80 wt % solution in toluene), K₂CO₃, DMF, 3 d; (j) **44**, Pd(dppf)Cl₂, CuI, NEt₃, DMF, 100 °C, 4 h; (k) TFA, 15 min; (l) (i) pyrrolidine, Cs₂CO₃, RuPhos, RuPhos Pd G1 methyl *tert*-butyl ether adduct, ^tBuOH, 85 °C, 15 h (ii) TFA, 30 min; (m) (i) 3-pyridinylboronic acid, Pd(dppf)Cl₂, K₂CO₃, dioxane, H₂O, 100 °C μW, 30 min (ii) TFA, 15 min; (n) B₂pin₂, Pd(dppf)Cl₂, KOAc, dioxane, 80 °C, 3 h; (o) (i) 3-(bromomethyl)pyridine HBr, Pd(PPh₃)₄, K₂CO₃, DME, H₂O, 95 °C, 10 h (ii) TFA, 30 min.

resultant product was taken forward crude in the synthesis of **24d** (18% yield overall) (Scheme 3). The nitrile group of **24d** was also hydrolyzed to an amide, affording **24e** (28% yield) (Scheme 3). Compounds **26c** and **26f** were synthesized in a similar manner to **25**, using the previously generated β-ketonitriles **55c** and **55f** from the production of **24c** and **24f** (Scheme 3). However, the intermediates from the reaction with trichloroacetonitrile were taken forward crude, after aqueous work up, to the subsequent reaction with hydrazine (45–62% yield overall).

The production of compounds **26g–m** and **27g** (Scheme 4) involved the synthesis of methyl esters **54g–i** and **54l–m** from

alkylation of indole **50** using a mixture of the corresponding electrophile with sodium hydride in DMF. Following the consumption of starting material, the reaction was diluted with methanol and sulfuric acid and heated at reflux to recover the carboxylic acid side-product. While the electrophiles for the synthesis of methyl esters **54g** and **54i** were commercially available, **54h–i** and **54m** required the synthesis of precursors. Alkyl halide **58** for **54i** was generated from alcohol **57** by treatment with tosyl chloride and DMAP (17% yield), itself produced by the reduction of ester **56** using lithium aluminium hydride (91% yield). Alcohol **60**, itself a product of the reduction of ester **59** using sodium borohydride (67% yield),

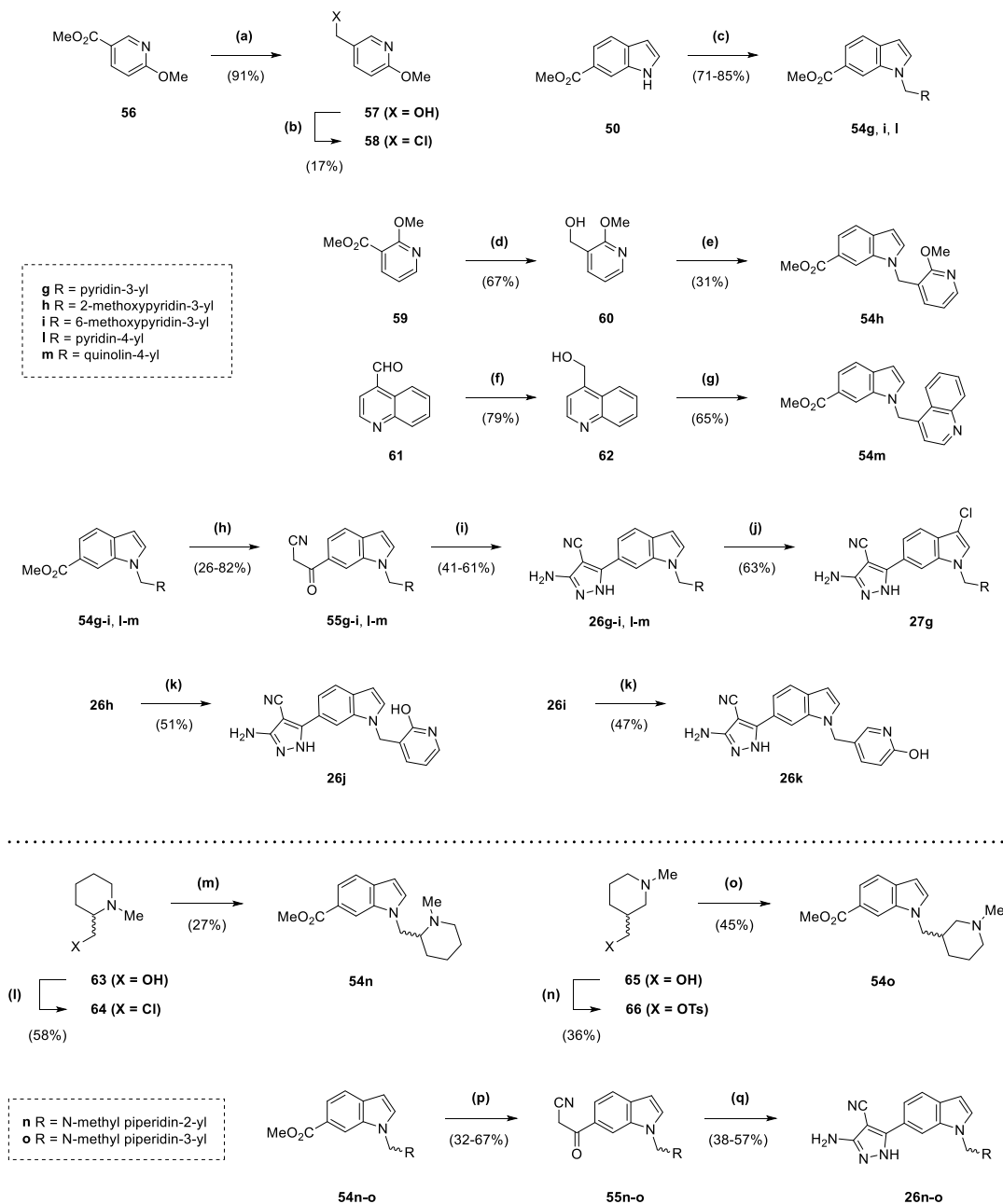
Scheme 3. Synthesis of Compounds 19, 23, 24a–f, 25, 26c, and 26f^a

^aReagents and conditions: (a) *n*-butyllithium (1.6 M in hexanes), acetonitrile, THF, -78°C , 30 min; (b) $\text{N}_2\text{H}_4\cdot\text{H}_2\text{O}$, EtOH, reflux, 6 h; (c) NaH, TBDMSCl, THF, 0°C to rt, 10 h; (d) (i) *n*-butyllithium (1.6 M in hexanes), acetonitrile, toluene, -78°C , 1 h (ii) TBAF (1 M in THF), THF, 20 min; (e) $\text{N}_2\text{H}_4\cdot\text{H}_2\text{O}$, EtOH, reflux, 12 h; (f) CCl_3CN , NaOAc, EtOH, 90 min; (g) $\text{N}_2\text{H}_4\cdot\text{H}_2\text{O}$, EtOH, reflux, 22 h; (h) RCH_2X ($\cdot\text{HX}$), Cs_2CO_3 , acetonitrile, reflux, 1–15 h; (i) *n*-butyllithium (1.6 M in hexanes), acetonitrile, toluene/THF, -78°C , 15 min to 1 h; (j) $\text{N}_2\text{H}_4\cdot\text{H}_2\text{O}$, EtOH, reflux, 5–13 h; (k) (i) *n*-butyllithium (1.6 M in hexanes), acetonitrile, toluene, -78°C , 1 h (ii) $\text{N}_2\text{H}_4\cdot\text{H}_2\text{O}$, EtOH, reflux, 5 h; (l) NaOH, H_2O , 100°C , 7 h; (m) (i) CCl_3CN , NaOAc, EtOH, 90 min to 9 h (ii) $\text{N}_2\text{H}_4\cdot\text{H}_2\text{O}$, EtOH, reflux, 5–15 h.

was treated with tosyl chloride in a similar manner to **57**; however, the product was taken forward crude for reaction with indole **50** to afford **54h** (31% yield overall). With **54m**, aldehyde **61** was reduced to the corresponding alcohol **62** by sodium borohydride (79% yield),²⁷ which was heated at reflux in aqueous HBr to afford a crude material that was taken forward for reaction with **50** (65% yield overall). The methyl esters **54g–i** and **54l–m** were converted to the corresponding β -ketonitriles **55g–i** and **55l–m** (26–82% yield), which were used to produce the 4-cyanopyrazole compounds in the same manner as **26c** and **26f** (41–61% yield overall). 2-Hydroxypyridyl/pyridone compounds **26j** and **26k** were synthesized from methoxypyridyl precursors **26h** and **26i**, respectively, using nucleophilic demethylation with lithium chloride and *p*-toluenesulfonic acid in DMF (47–51% yield).²⁸ Meanwhile, 3-chloroindole derivative **27g** was synthesized directly from **26g** through treatment with *N*-chlorosuccinimide in DMF (63% yield). Synthesis of compounds **26n** and **26o** (Scheme 4) began with conversion of racemic alcohols **63** and **65**, respectively, to electrophilic alkylating agents. Alkyl chloride **64** was produced

from **63** using thionyl chloride (58% yield), while treatment of **65** with tosyl chloride, triethylamine, and DMAP generated the alkyl tosylate **66** (36% yield). Synthesis of the methyl esters **54n–o** from indole **50** and the agents **64** and **66** with sodium hydride in DMF involved heating at 60°C (27–45% yield), with NaI also added as a catalyst for **54o**. These esters were converted to the corresponding β -ketonitriles **55n–o** (32–67% yield), which were used to produce the 4-cyanopyrazole compounds in the same manner as **26c** and **26f** (38–57% yield overall).

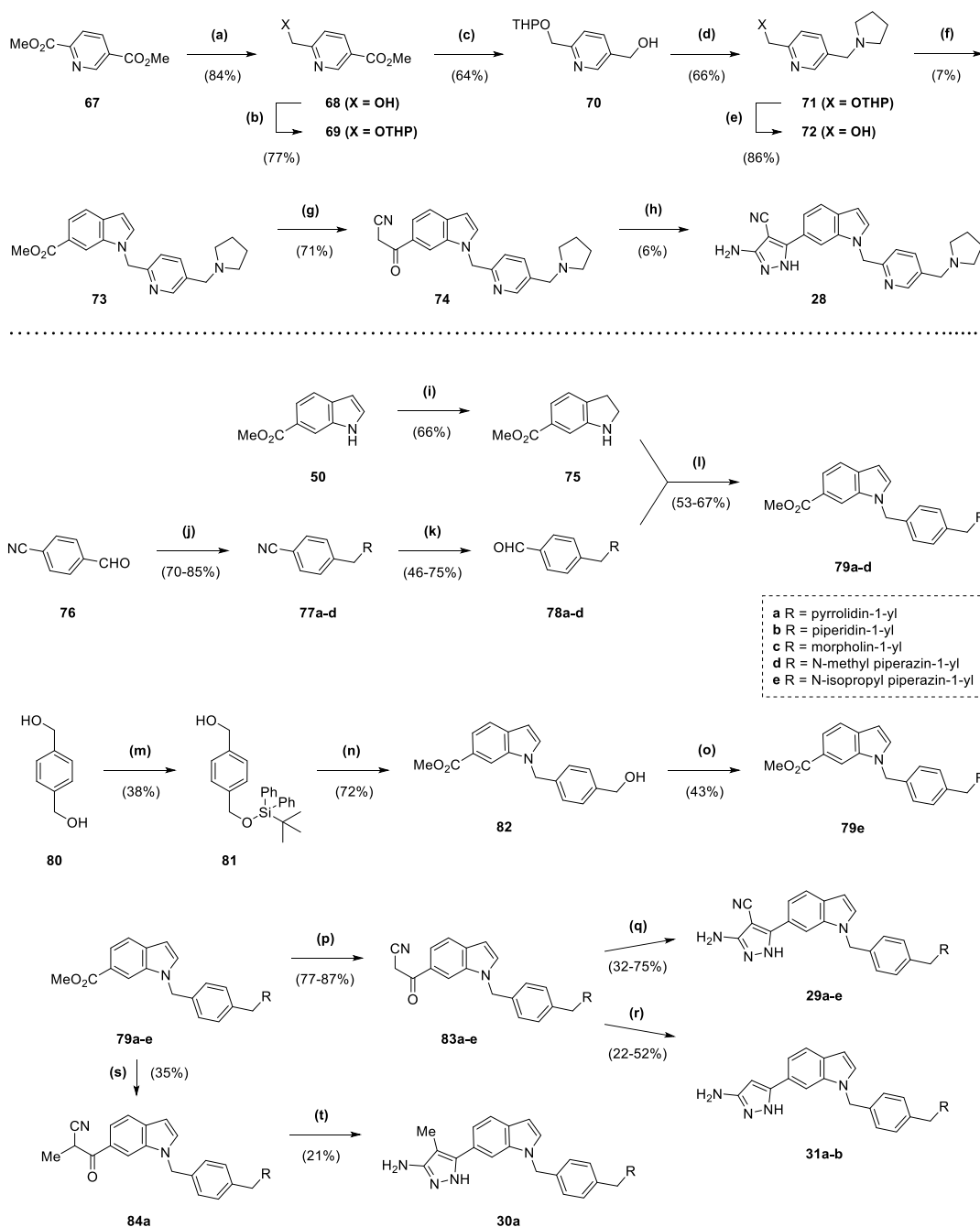
Synthesis of **28** (Scheme 5) began with regioselective reduction of diester **67** using a combination of sodium borohydride and CaCl_2 (84% yield),²⁹ with protection of the resultant alcohol **68** as a tetrahydropyranyl ether in **69** (77% yield). The ester of **69** was reduced with lithium aluminium hydride to the corresponding alcohol **70** (64% yield), which was converted to a mesylate then reacted with pyrrolidine and Cs_2CO_3 in DMF to afford **71** (66% yield overall). The tetrahydropyranyl ether **71** was deprotected with *p*-toluenesulfonic acid in ethanol (86% yield), and the resultant alcohol **72** converted to a mesylate that was reacted with indole **50** using

Scheme 4. Synthesis of Compounds 26g–o and 27g^a

^aReagents and conditions: (a) LiAlH_4 , THF, 0 °C, 1 h; (b) TsCl, DMAP, NEt_3 , DCM, 18 h; (c) (i) $\text{RCH}_2\text{X}\cdot\text{HX}$ (**58** for **54i**), NaH, DMF, 0 °C to rt, 45 min to 1 h (ii) MeOH, H_2SO_4 , reflux, 1–16 h; (d) NaBH_4 , EtOH, 0 °C to rt, 1 d; (e) (i) TsCl, DMAP, NEt_3 , DCM, 2 h (ii) **50**, NaH, DMF, 0 °C to rt, 30 min (iii) MeOH, H_2SO_4 , reflux, 90 min; (f) NaBH_4 , MeOH, 0 °C, 90 min; (g) (i) aqueous HBr (48%), reflux, 90 min (ii) **50**, NaH, DMF, 0 °C to rt, 15 min (iii) MeOH, H_2SO_4 , reflux, 2 h; (h) *n*-butyllithium (1.6 M in hexanes), acetonitrile, toluene/THF, –78 °C, 30 min to 1 h; (i) (i) CCl_3CN , NaOAc, EtOH, 13–36 h (ii) $\text{N}_2\text{H}_4\cdot\text{H}_2\text{O}$, EtOH, reflux, 6–21 h; (j) NCS, DMF, 7 h 30 min; (k) LiCl, TsOH· H_2O , DMF, 120 °C, 25 min; (l) SOCl_2 , DCM, reflux, 7 h; (m) **50**, NaH, DMF, 0–60 °C, 1 h (ii) MeOH, H_2SO_4 , reflux, 1 h; (n) TsCl, DMAP, NEt_3 , DCM, 4 h; (o) (i) **50**, NaH, NaI, DMF, 0–60 °C, 1 h; (p) *n*-butyllithium (1.6 M in hexanes), acetonitrile, THF, –78 °C, 30 min to 1 h; (q) (i) CCl_3CN , NaOAc, EtOH, 3 h 30 min to 18 h (ii) $\text{N}_2\text{H}_4\cdot\text{H}_2\text{O}$, EtOH, reflux, 15 h to 1 d.

sodium hydride and NaI in DMF at elevated temperatures (7% yield overall). The methyl ester **73** was converted to the corresponding β -ketonitrile **74** (71% yield), which was used to produce **28** in the same manner as **26c** and **26f** (6% yield overall). Compounds **29a–e** (Scheme 5) were all produced from methyl esters **79a–e**. Esters **79a–d** were synthesized by the microwave-assisted condensation of aldehydes **78a–d** and indoline **75** (53–67% yield),³⁰ itself produced by the reduction of indole **50** using sodium cyanoborohydride in acetic acid (66%

yield).³¹ Aldehydes **78a–d** were generated in two steps by reductive amination of 4-cyanobenzaldehyde **76** with various secondary amines to form **77a–d** (70–85% yield), followed by reduction using diisobutylaluminum hydride (46–75% yield). In comparison, ester **79e** required the protection of one of the alcohols of **80** with a *tert*-butyldiphenylsilyl group (38% yield), followed by conversion of the remaining alcohol of **81** to a crude mixture of the mesylate and chloride that was used to alkylate **50** with sodium hydride and DMF, with subsequent deprotection of

Scheme 5. Synthesis of Compounds 28, 29a–e, 30a, and 31a–b^a

^aReagents and conditions: (a) NaBH_4 , CaCl_2 , MeOH, THF, 0 °C, 90 min; (b) MsOH, 3,4-dihydro-2H-pyran, DCM, 150 min; (c) LiAlH_4 , THF, 0 °C, 45 min; (d) (i) MsCl, NEt_3 , DCM, 0 °C to rt, 1 h (ii) pyrrolidine, Cs_2CO_3 , DMF, 14 h; (e) TsOH· H_2O , ethanol, 50 °C, 30 min; (f) (i) MsCl, NEt_3 , DCM, 0 °C to rt, 150 min; (ii) **50**, NaH, NaI, DMF, 0 to 60 °C, 75 min (iii) MeOH, H_2SO_4 , reflux, 14 h; (g) *n*-butyllithium (1.6 M in hexanes), acetonitrile, THF, -78 °C, 1 h; (h) (i) CCl_3CN , NaOAc, EtOH, 36 h (ii) $\text{N}_2\text{H}_4\cdot\text{H}_2\text{O}$, EtOH, reflux, 1 d; (i) NaCNBH_3 , AcOH, 0 °C to rt, 7 h; (j) $\text{Na}(\text{OAc})_3\text{BH}$, RH, AcOH, DCM, 80 min to 15 h; (k) DIBAL-H, THF, 0 °C to rt, 90 min to 1 h; (l) PhCO_2H , toluene, 200 °C μW , 20–30 min; (m) TBDPSCl, imidazole, DMF, 21 h; (n) (i) MsCl, NEt_3 , DCM, 0 °C to rt, 1 h (ii) **50**, NaH, DMF, 0 °C to rt, 45 min (iii) TBAF (1 M in THF), 30 min; (o) (i) MsCl, NEt_3 , DCM, 0 °C to rt, 90 min (ii) RH, Cs_2CO_3 , DMF, 12 h; (p) *n*-butyllithium (1.6 M in hexanes), acetonitrile, THF, -78 °C, 20 min to 1 h; (q) (i) CCl_3CN , NaOAc, EtOH, 4 h to 2 d (ii) $\text{N}_2\text{H}_4\cdot\text{H}_2\text{O}$, EtOH, reflux, 7 h to 1 d; (r) $\text{N}_2\text{H}_4\cdot\text{H}_2\text{O}$, EtOH, reflux, 12–21 h; (s) *n*-butyllithium (1.6 M in hexanes), propionitrile, toluene, -78 to 0 °C, 2 h; (t) $\text{N}_2\text{H}_4\cdot\text{H}_2\text{O}$, EtOH, reflux, 1 d.

the silyl protecting group with TBAF (72% yield overall). The benzyl alcohol of **82** was treated with mesyl chloride and triethylamine, then functionalized with 1-isopropylpiperazine to afford **79e** (43% yield overall). The methyl esters **79a–e** were converted to the corresponding β -ketonitriles **83a–e** (77–87% yield), which were used to produce **29a–e** in the same manner

as **26c** and **26f** (32–75% yield overall) or **31a–b** by heating at reflux with hydrazine in ethanol (22–52% yield). Methyl ester **79a** was also used to produce **30a** (Scheme 5) through initial treatment with *n*-butyllithium and propionitrile to afford β -ketonitrile **84a** (35% yield), which was then heated at reflux with hydrazine in ethanol (21% yield).

Table 7. Minimum Inhibitory Concentrations (MIC) against *Mab* and *Mtb* of Compounds 26l, 28, 29a–e, and 31a–b

compound	<i>Mab</i> TrmD K_d (μ M)	<i>Mab</i> MIC (μ M)	H37Rv <i>Mtb</i> MIC (μ M)			
			GAST-Fe	7H9/ADC	7H9/glucose	7H9/DPPC
26l	0.12 \pm 0.02	50	50	>100	ND	ND
28	0.092 \pm 0.018	50	ND	ND	ND	ND
29a ^a	0.027 \pm 0.004	50	50	>100	25	12.5
29b	0.070 \pm 0.029	50	50	100	25	12.5
29c	0.19 \pm 0.02	50	50	>100	100	50
29d ^a	0.073 \pm 0.030	50	25	50	12.5	6.3
29e	0.10 \pm 0.02	50	6.3	12.5	2.3	1.6
31a ^a	0.49 \pm 0.21	50	25	100	12.5	6.3
31b	0.71 \pm 0.09	50	50	>100	25	12.5

^a*Mab* MIC and H37Rv *Mtb* MIC (7H9/DPPC) previously reported.¹²

Screening of Compounds against Mycobacteria. The effect of compounds on *Mab* and *Mtb* growth in liquid culture was determined and revealed promising minimal inhibitory concentrations (MIC) for many compounds (Table 7). A lack of correlation between target binding affinity and activity against bacteria was observed, indicating likely effects of differential permeability, retention, and metabolism of compounds on their in vitro activity. While compounds performed similarly against *Mab*, 29e afforded the best results against *Mtb* across different media types and carbon sources, with MIC values of 1.6 and 2.3 μ M achieved with 7H9 supplemented by dipalmitoyl phosphatidylcholine (DPPC) and glucose respectively. Both glucose and DPPC are carbon sources predicted to be relevant during the in vivo pathogenesis of *Mtb*,³² and the activity of the compounds during catabolism of both of these supports the notion that TrmD inhibition will inhibit bacterial growth under any metabolic condition. The poor activity in 7H9/ADC was likely due to high protein binding because this medium contains 0.4% bovine serum albumin. Hence, overcoming protein binding will be an important component of future drug design strategies.

In addition to the results against *Mab* and *Mtb* in liquid culture, activity was observed by compounds from the lead series in macrophage infection models against *Mab* and *M. leprae*, demonstrating the utility of the series against mycobacteria in vivo.¹²

CONCLUSIONS

With the application of a fragment-growing approach to a highly ligand-efficient fragment hit of *Mab* TrmD failing to afford a significant improvement in binding affinity, a fragment-merging approach was explored. The combination of structural features of two fragments, 16 (K_d 170 μ M, LE 0.37) and 20 (K_d 0.26 mM, LE 0.41), proved promising with the resultant aminopyrazole-indole compound 23 (K_d 110 μ M, LE 0.36) possessing improved affinity. Controlled elaboration with 23, guided by extensive structural information and biophysical data, resulted in the development of a ligand-efficient low-nanomolar affinity compound 29a (K_d 27 nM, LE 0.34) against *Mab* TrmD. Compounds from this fragment-merging series were subsequently screened against both *Mab* and *Mtb* growth in liquid culture, with many affording promising MIC values. These results are encouraging and support the use of TrmD as a target for the development of compounds with antimycobacterial activity. As a result, the work described in this study is currently being developed in the pursuit of further compounds with potent activity against *Mab*.

EXPERIMENTAL SECTION

General Chemistry. All reactions were carried out in oven-dried glassware under a positive pressure of dry nitrogen atmosphere. Temperatures of 0 and -78 °C were obtained by submerging the reaction vessel in a bath containing either ice or a mixture of solid CO₂ pellets and acetone respectively. The solvents dichloromethane (DCM), ethyl acetate, acetonitrile, methanol, petroleum ether, and toluene were distilled over calcium hydride under a dry nitrogen atmosphere prior to use, with tetrahydrofuran (THF) distilled over a mixture of lithium aluminium hydride, calcium hydride, and triphenylphosphine. DMF was purchased as anhydrous from commercial suppliers, with ethanol and acetic acid obtained in the absolute and glacial forms, respectively. All purchased chemicals were used as received. Solutions of Na₂CO₃, NaHCO₃, NaCl (brine), and NH₄Cl were aqueous and saturated. Solutions of LiCl were aqueous and 5% w/v.

Flash column chromatography was performed using automated Biotage Isolera Spektra purification systems with appropriately sized Biotage SNAP cartridges, containing either KP 50 μ m silica in “normal phase” purification or HP-sphere 25 μ m C18 silica in “reverse phase” purification. Microwave heating was performed using a Biotage Initiator + system with sealed Biotage microwave reaction vials. Analytical thin layer chromatography (TLC) was performed using Merck glass-backed silica plates, with visualization by 254 or 365 nm ultraviolet light.

Liquid chromatography mass spectrometry (LCMS) was carried out using a Waters Acquity UPLC H-Class system, with samples run on a solvent gradient from 0 to 95% acetonitrile in water (+0.1% formic acid) over 4 min. Peaks corresponding to the desired product are described, including the retention time (rt) and % purity by integration. High resolution mass spectrometry (HRMS) was mainly performed using ThermoFinnigan Orbitrap Classic, Waters LCT Premier or Waters Vion IMS QToF systems. A PerkinElmer Spectrum One FT-IR spectrometer fitted with a universal attenuated total reflectance accessory was used to record infrared spectra, with wavenumbers of maximum absorbance (ν_{max}) quoted in wavenumbers (cm⁻¹) for signals outside of the fingerprint region (br = broad). Only peaks corresponding to key functional groups were characterized. Nuclear magnetic resonance (NMR) spectra were recorded in the indicated deuterated solvents with Avance III HD (400 MHz), QNP Cryoprobe (400 MHz), or DCH Cryoprobe (500 MHz) Bruker spectrometers. ¹H NMR data are presented in the following order: chemical shift (in ppm on a δ scale relative to the residual solvent resonance peak), integration, multiplicity (s = singlet, d = doublet, t = triplet, q = quartet, quin = quintet, sep = septet, m = multiplet), and coupling constant (*J*, in Hz). ¹³C NMR spectra were proton-decoupled, with chemical shifts recorded, and further description are provided for certain peaks (br = broad).

A combination of TLC and LCMS analysis was used to monitor reactions. All tested compounds possessed a purity of at least 95% as determined by LCMS analysis (except for compound 2, for which LCMS analysis was not possible).

The synthesis of **23**, **24f**, **26f**, **28**, **29a**, **29d**, and **31a**, and associated intermediates including **51**, **52**, **54f**, **55f**, **68–75**, **77a**, **77d**, **78a**, **78d**, **79a**, **79d**, **83a**, and **83d**, have previously been reported.¹²

N-Ethyl-1H-pyrazole-4-carboxamide (2). Palladium on carbon (10 wt % loading, 0.150 g) was added to a suspension of 1-benzyl-N-ethyl-1H-pyrazole-4-carboxamide **34** (75 mg, 0.33 mmol) in *tert*-butanol (15 mL) and formic acid (1.5 mL). The reaction mixture was heated to 50 °C over 2 h, then filtered, and concentrated in vacuo. Purification by flash column chromatography (0–15% methanol in DCM) afforded **2** (29 mg, 64% yield). ¹H NMR: (400 MHz, CD₃OD) 8.03 (2H, s), 3.36 (2H, q, *J* = 7.3 Hz), 1.20 (3H, t, *J* = 7.3 Hz); ¹³C NMR: (100 MHz, CD₃OD) 165.3, 119.1, 35.2, 15.0 (1 peak missing); $\nu_{\max}/\text{cm}^{-1}$: 3302 (N–H), 3110, 2974, 2876, 1632 (C=O), 1584, 1541, 1515; HRMS (ESI)⁺: *m/z* calcd for [C₆H₉N₃O + H]⁺, 140.0818; observed, 140.0818.

Benzyl 1H-Pyrazole-4-carboxylate (3). Benzyl bromide (0.11 mL, 0.92 mmol) and *N,N*-diisopropylethylamine (0.20 mL, 1.1 mmol) were added to a solution of 1-(tetrahydro-2H-pyran-2-yl)-1H-pyrazole-4-carboxylic acid **36** (0.150 g, 0.765 mmol) in DMF (2.5 mL). The reaction mixture was stirred over 2 h, then diluted with ethyl acetate (200 mL), washed with LiCl solution (2 × 100 mL) and brine (2 × 200 mL), dried (MgSO₄), and concentrated in vacuo to afford the crude reaction intermediate. TFA (1 mL) was added, and the reaction mixture was stirred over 12 min, then diluted with NaHCO₃ solution (20 mL) at 0 °C, and extracted into DCM (3 × 50 mL). The combined organic extracts were washed with NaHCO₃ solution (50 mL) and brine (50 mL), dried (MgSO₄), and concentrated in vacuo. Purification by flash column chromatography (0–85% ethyl acetate in petroleum ether) afforded **3** (76 mg, 50% yield). LCMS (ESI)⁺: *m/z* 203.2 [M + H]⁺, (ESI)[−]: *m/z* 201.1 [M − H][−], rt 1.61 min, >99%; ¹H NMR: (500 MHz, CDCl₃) 10.83 (1H, br s), 8.09 (2H, s), 7.45–7.32 (5H, m), 5.31 (2H, s); ¹³C NMR: (125 MHz, CDCl₃) 163.0, 136.8 (br), 136.2, 128.7, 128.41, 128.36, 115.1, 66.2; $\nu_{\max}/\text{cm}^{-1}$: 3168, 3124, 3043, 2947, 2835, 1714, 1702 (C=O), 1578, 1521; HRMS (ESI)⁺: *m/z* calcd for [C₁₁H₁₀N₂O₂ + H]⁺, 203.0815; observed, 203.0823.

4-Nitrobenzyl 1H-Pyrazole-4-carboxylate (4). EDC·HCl (0.293 g, 1.53 mmol) was added to a solution of 1-(tetrahydro-2H-pyran-2-yl)-1H-pyrazole-4-carboxylic acid **36** (0.200 g, 1.02 mmol), 4-nitrobenzyl alcohol (0.188 g, 1.22 mmol), *N,N*-diisopropylethylamine (0.267 mL, 1.53 mmol), and DMAP (19 mg, 0.15 mmol) in DCM (5 mL). The reaction mixture was stirred overnight, then diluted with water (30 mL), and extracted into DCM (3 × 20 mL). The combined organic extracts were washed (brine), dried (MgSO₄), and concentrated in vacuo. Purification by flash column chromatography (30–80% ethyl acetate in petroleum ether) afforded the reaction intermediate. TFA (2 mL) was added to a solution of the reaction intermediate in DCM (4 mL). The reaction mixture was stirred over 5 min, then diluted with NaHCO₃ solution (50 mL) at 0 °C, and extracted into DCM (3 × 50 mL). The combined organic extracts were washed (brine), dried (MgSO₄), and concentrated in vacuo. Purification by flash column chromatography (0–7% methanol in DCM) afforded **4** (98 mg, 40% yield). LCMS (ESI)[−]: *m/z* 246.1 [M − H][−], rt 1.62 min, >99%; ¹H NMR: (400 MHz, CDCl₃) 8.27–8.22 (2H, m), 8.11 (2H, s), 7.58 (2H, d, *J* = 8.9 Hz), 5.40 (2H, s); ¹³C NMR: (100 MHz, CDCl₃) 162.6, 147.9, 143.5, 136.9, 128.5, 124.0, 114.4, 64.7; $\nu_{\max}/\text{cm}^{-1}$: 3120, 2930, 2855, 1715 (C=O), 1606, 1518 (N–O), 1342 (N–O); HRMS (ESI)[−]: *m/z* calcd for [C₁₁H₉N₃O₄ − H][−], 246.0520; observed, 246.0512.

4-(Methoxycarbonyl)benzyl 1H-Pyrazole-4-carboxylate (5). Methyl-4-(bromomethyl) benzoate (0.248 g, 1.08 mmol) and *N,N*-diisopropylethylamine (0.24 mL, 1.5 mmol) were added to a solution of 1-(tetrahydro-2H-pyran-2-yl)-1H-pyrazole-4-carboxylic acid **36** (0.177 g, 0.903 mmol) in DMF (3 mL). The reaction mixture was stirred over 2 h, then diluted with ethyl acetate (200 mL), washed with LiCl solution (2 × 100 mL) and brine (2 × 200 mL), dried (MgSO₄), and concentrated in vacuo to afford the crude reaction intermediate. TFA (2 mL) was added, and the reaction mixture was stirred over 10 min, then diluted with NaHCO₃ solution (50 mL) at 0 °C, and extracted into DCM (3 × 50 mL). The combined organic extracts were washed with NaHCO₃ solution (50 mL) and brine (50 mL), dried (MgSO₄), and

concentrated in vacuo. Purification by flash column chromatography (0–70% ethyl acetate in petroleum ether) afforded **5** (0.115 g, 49% yield). LCMS (ESI)[−]: *m/z* 259.1 [M − H][−], rt 1.62 min, >99%; ¹H NMR: (400 MHz, CDCl₃) 8.10 (2H, s), 8.08–8.02 (2H, m), 7.48 (2H, d, *J* = 8.2 Hz), 5.36 (2H, s), 3.92 (3H, s); ¹³C NMR: (100 MHz, CDCl₃) 166.9, 162.8, 141.2, 136.9, 130.1, 130.0, 127.8, 114.7, 65.4, 52.4; $\nu_{\max}/\text{cm}^{-1}$: 3114, 2950, 1712 (C=O), 1617, 1578, 1523; HRMS (ESI)[−]: *m/z* calcd for [C₁₃H₁₂N₂O₄ + H]⁺, 261.0870; observed, 261.0860.

3-Cyanobenzyl 1H-Pyrazole-4-carboxylate (6). 3-(Bromomethyl)benzonitrile (0.360 g, 1.84 mmol) and *N,N*-diisopropylethylamine (0.53 mL, 3.1 mmol) were added to a solution of 1-(tetrahydro-2H-pyran-2-yl)-1H-pyrazole-4-carboxylic acid **36** (0.300 g, 1.53 mmol) in DMF (3.5 mL). The reaction mixture was stirred over 90 min, then diluted with ethyl acetate (200 mL), washed with LiCl solution (2 × 100 mL) and brine (2 × 200 mL), dried (MgSO₄), and concentrated in vacuo to afford the crude reaction intermediate. TFA (2 mL) was added, and the reaction mixture was stirred over 10 min, then diluted with NaHCO₃ solution (50 mL) at 0 °C, and extracted into DCM (3 × 50 mL). The combined organic extracts were washed with NaHCO₃ solution (50 mL) and brine (50 mL), dried (MgSO₄), and concentrated in vacuo. Purification by flash column chromatography (0–10% methanol in DCM) afforded **6** (0.197 g, 57% yield). LCMS (ESI)[−]: *m/z* 226.1 [M − H][−], rt 1.54 min, 96%; ¹H NMR: (500 MHz, CDCl₃) 8.10 (2H, s), 7.74–7.70 (1H, m), 7.67–7.61 (2H, m), 7.50 (1H, t, *J* = 7.8 Hz), 5.32 (2H, s); ¹³C NMR: (125 MHz, CDCl₃) 162.6, 137.8, 136.9, 132.5, 132.0, 131.6, 129.6, 118.6, 114.4, 113.0, 64.8; $\nu_{\max}/\text{cm}^{-1}$: 3179, 3125, 2951, 2227 (C≡N), 1721 (C=O), 1576, 1522; HRMS (ESI)[−]: *m/z* calcd for [C₁₂H₉N₃O₂ + H]⁺, 228.0768; observed, 228.0782.

3-Methoxybenzyl 1H-Pyrazole-4-carboxylate (7). 3-Methoxybenzyl bromide (0.13 mL, 0.92 mmol) and *N,N*-diisopropylethylamine (0.20 mL, 1.1 mmol) were added to a solution of 1-(tetrahydro-2H-pyran-2-yl)-1H-pyrazole-4-carboxylic acid **36** (0.150 g, 0.765 mmol) in DMF (2.5 mL). The reaction mixture was stirred over 2 h, then diluted with ethyl acetate (200 mL), washed with LiCl solution (2 × 100 mL) and brine (2 × 200 mL), dried (MgSO₄), and concentrated in vacuo. Purification by flash column chromatography (0–85% ethyl acetate in petroleum ether) afforded the reaction intermediate. TFA (1 mL) was added, and the reaction mixture was stirred over 10 min, then diluted with NaHCO₃ solution (20 mL) at 0 °C, and extracted into DCM (3 × 15 mL). The combined organic extracts were washed with NaHCO₃ solution (50 mL) and brine (50 mL), dried (MgSO₄), and concentrated in vacuo. Purification by flash column chromatography (30–60% ethyl acetate in petroleum ether) afforded **7** (8.2 mg, 5% yield). LCMS (ESI)[−]: *m/z* 231.2 [M − H][−], rt 1.64 min, 98%; ¹H NMR: (400 MHz, CDCl₃) 8.09 (2H, s), 7.30 (1H, t, *J* = 7.9 Hz), 7.00 (1H, d, *J* = 7.7 Hz), 6.97–6.93 (1H, m), 6.88 (1H, dd, *J* = 8.1, 2.5 Hz), 5.28 (2H, s), 3.82 (3H, s); ¹³C NMR: (100 MHz, CDCl₃) 162.9, 159.9, 137.7, 136.9, 129.8, 120.5, 115.0, 113.9, 113.8, 66.1, 55.4; $\nu_{\max}/\text{cm}^{-1}$: 3276, 3113, 2942, 1718, 1678 (C=O), 1598, 1558; HRMS (ESI)[−]: *m/z* calcd for [C₁₂H₁₂N₂O₃ + H]⁺, 233.0921; observed, 233.0927.

3-(2-Methoxy-2-oxoethoxy)benzyl 1H-Pyrazole-4-carboxylate (8). Caesium carbonate (0.336 g, 1.03 mmol) and methyl bromoacetate (54 μL, 0.57 mmol) were added to a solution of 3-hydroxybenzyl 1-(tetrahydro-2H-pyran-2-yl)-1H-pyrazole-4-carboxylate **40** (0.156 mg, 0.516 mmol) in DMF (3 mL). The reaction mixture was stirred over 2 h, then diluted with ethyl acetate (200 mL), washed with LiCl solution (2 × 100 mL) and brine (2 × 200 mL), dried (MgSO₄), and concentrated in vacuo to afford the crude reaction intermediate. TFA (2 mL) was added, and the reaction mixture was stirred over 15 min, then diluted with NaHCO₃ solution (50 mL) at 0 °C, and extracted into DCM (3 × 50 mL). The combined organic extracts were washed with NaHCO₃ solution (50 mL) and brine (50 mL), dried (MgSO₄), and concentrated in vacuo. Purification by flash column chromatography (0–100% ethyl acetate in petroleum ether) afforded **8** (75 mg, 50% yield). LCMS (ESI)⁺: *m/z* 291.2 [M + H]⁺, (ESI)[−]: *m/z* 289.1 [M − H][−], rt 1.61 min, >99%; ¹H NMR: (400 MHz, CDCl₃) 10.75 (1H, br s), 8.08 (2H, s), 7.30 (1H, t, *J* = 7.9 Hz), 7.05 (1H, d, *J* = 7.5 Hz), 6.98 (1H, s), 6.86 (1H, dd, *J* = 8.2, 2.2 Hz), 5.27

(2H, s), 4.65 (2H, s), 3.80 (3H, s); ^{13}C NMR: (100 MHz, CDCl_3) 169.5, 162.9, 158.1, 138.0, 137.0 (br), 130.0, 121.6, 114.9, 114.6, 114.3, 65.8, 65.5, 52.5; $\nu_{\text{max}}/\text{cm}^{-1}$: 3303, 1745 (C=O), 1714 (C=O), 1587, 1561; HRMS (ESI) $^+$: m/z calcd for $[\text{C}_{14}\text{H}_{14}\text{N}_2\text{O}_5 + \text{Na}]^+$, 313.0795; observed, 313.0792.

3-(Pyridin-2-ylmethoxy)benzyl 1H-Pyrazole-4-carboxylate (9). Caesium carbonate (0.970 g, 2.98 mmol) and 2-bromomethylpyridine hydrobromide (0.282 g, 1.09 mmol) were added to a solution of 3-hydroxybenzyl 1-(tetrahydro-2H-pyran-2-yl)-1H-pyrazole-4-carboxylate **40** (0.300 g, 0.992 mmol) in DMF (3.5 mL). The reaction mixture was stirred over 2 h, then diluted with ethyl acetate (80 mL), washed with LiCl solution (2 \times 100 mL) and brine (2 \times 150 mL), dried (MgSO_4), and concentrated in vacuo to afford the crude reaction intermediate. TFA (2 mL) was added, and the reaction mixture was stirred over 15 min, then diluted with NaHCO_3 solution (50 mL) at 0 $^\circ\text{C}$, and extracted into DCM (3 \times 50 mL). The combined organic extracts were washed with NaHCO_3 solution (50 mL) and brine (50 mL), dried (MgSO_4), and concentrated in vacuo. Purification by flash column chromatography (20–100% ethyl acetate in petroleum ether) afforded **9** (0.163 g, 53% yield). LCMS (ESI) $^+$: m/z 310.2 $[\text{M} + \text{H}]^+$, (ESI) $^-$: m/z 308.1 $[\text{M} - \text{H}]^-$, rt 1.55 min, 97%; ^1H NMR: (400 MHz, CDCl_3) 11.01 (1H, br s), 8.59 (1H, d, $J = 4.8$ Hz), 8.08 (2H, s), 7.72 (1H, td, $J = 7.7, 1.7$ Hz), 7.52 (1H, d, $J = 7.8$ Hz), 7.29 (1H, t, $J = 7.9$ Hz), 7.23 (1H, dd, $J = 7.1, 5.1$ Hz), 7.08–7.04 (1H, m), 7.01 (1H, d, $J = 7.7$ Hz), 6.95 (1H, dd, $J = 8.2, 2.2$ Hz), 5.27 (2H, s), 5.22 (2H, s); ^{13}C NMR: (100 MHz, CDCl_3) 162.9, 158.7, 157.2, 149.3, 137.9, 137.1, 129.9, 122.9, 121.5, 120.9, 114.9, 114.7, 114.6, 70.7, 65.9 (1 peak missing); $\nu_{\text{max}}/\text{cm}^{-1}$: 3118, 2947, 1707 (C=O), 1598, 1570, 1516; HRMS (ESI) $^-$: m/z calcd for $[\text{C}_{17}\text{H}_{15}\text{N}_3\text{O}_3 - \text{H}]^-$, 308.1041; observed, 308.1030.

3-Ethoxybenzyl 1H-Pyrazole-4-carboxylate (10). Triphenylphosphine (0.217 g, 0.831 mmol), ethanol (49 μL , 0.83 mmol), and diisopropyl azodicarboxylate (0.16 mL, 0.83 mmol) were added to a solution of 3-hydroxybenzyl 1-(tetrahydro-2H-pyran-2-yl)-1H-pyrazole-4-carboxylate **40** (0.250 g, 0.831 mmol) in THF (5 mL). The reaction mixture was stirred over 1 h, then diluted with NaHCO_3 solution (35 mL), and extracted into diethyl ether (3 \times 30 mL). The combined organic extracts were washed with NaHCO_3 solution (40 mL) and brine (40 mL), dried (Na_2SO_4), and concentrated in vacuo. Purification by flash column chromatography (20–100% ethyl acetate in petroleum ether) afforded the reaction intermediate. TFA (2 mL) was added, and the reaction mixture was stirred over 15 min, then diluted with NaHCO_3 solution (50 mL) at 0 $^\circ\text{C}$, and extracted into DCM (3 \times 50 mL). The combined organic extracts were washed (brine), dried (MgSO_4), and concentrated in vacuo. Purification by flash column chromatography (0–90% ethyl acetate in petroleum ether) afforded **10** (94 mg, 46% yield). LCMS (ESI) $^+$: m/z 247.2 $[\text{M} + \text{H}]^+$, (ESI) $^-$: m/z 245.1 $[\text{M} - \text{H}]^-$, rt 1.79 min, >99%; ^1H NMR: (500 MHz, CDCl_3) 8.09 (2H, s), 7.28 (1H, t, $J = 7.9$ Hz), 6.98 (1H, d, $J = 7.5$ Hz), 6.96–6.94 (1H, m), 6.86 (1H, dd, $J = 8.2, 2.4$ Hz), 5.27 (2H, s), 4.04 (2H, q, $J = 7.0$ Hz), 1.41 (3H, t, $J = 7.0$ Hz); ^{13}C NMR: (125 MHz, CDCl_3) 163.0, 159.3, 137.6, 136.9, 129.8, 120.4, 115.0, 114.4, 114.3, 66.1, 63.6, 15.0; $\nu_{\text{max}}/\text{cm}^{-1}$: 3256, 3118, 2979, 2942, 2888, 1686 (C=O), 1601, 1559; HRMS (ESI) $^+$: m/z calcd for $[\text{C}_{13}\text{H}_{14}\text{N}_2\text{O}_3 + \text{H}]^+$, 247.1077; observed, 247.1084.

3-Phenethoxybenzyl 1H-Pyrazole-4-carboxylate (11). Triphenylphosphine (0.261 g, 0.997 mmol), phenethyl alcohol (0.12 mL, 1.0 mmol), and diisopropyl azodicarboxylate (0.20 mL, 1.0 mmol) were added to a solution of 3-hydroxybenzyl 1-(tetrahydro-2H-pyran-2-yl)-1H-pyrazole-4-carboxylate **40** (0.300 g, 0.997 mmol) in THF (5 mL). The reaction mixture was stirred overnight, then diluted with NaHCO_3 solution (30 mL), and extracted into diethyl ether (3 \times 30 mL). The combined organic extracts were washed with NaHCO_3 solution (40 mL) and brine (40 mL), dried (Na_2SO_4), and concentrated in vacuo. Purification by flash column chromatography (0–100% ethyl acetate in petroleum ether) afforded the reaction intermediate. TFA (2 mL) was added, and the reaction mixture was stirred over 15 min, then diluted with NaHCO_3 solution (50 mL) at 0 $^\circ\text{C}$, and extracted into DCM (3 \times 50 mL). The combined organic extracts were washed with NaHCO_3 solution (50 mL) and brine (50

mL), dried (MgSO_4), and concentrated in vacuo. Purification by flash column chromatography (0–100% ethyl acetate in petroleum ether) afforded **11** (77 mg, 24% yield). LCMS (ESI) $^+$: m/z 323.2 $[\text{M} + \text{H}]^+$, (ESI) $^-$: m/z 321.1 $[\text{M} - \text{H}]^-$, rt 2.08 min, >99%; ^1H NMR: (500 MHz, CDCl_3) 10.69 (1H, br s), 8.08 (2H, s), 7.35–7.21 (6H, m), 7.01–6.97 (1H, m), 6.95 (1H, t, $J = 1.9$ Hz), 6.87 (1H, ddd, $J = 8.3, 2.5, 0.7$ Hz), 5.26 (2H, s), 4.19 (2H, t, $J = 7.1$ Hz), 3.10 (2H, t, $J = 7.1$ Hz); ^{13}C NMR: (125 MHz, CDCl_3) 162.9, 159.1, 138.3, 137.7, 136.9, 129.8, 129.1, 128.7, 126.7, 120.6, 115.0, 114.6, 114.4, 68.8, 66.1, 35.9; $\nu_{\text{max}}/\text{cm}^{-1}$: 1714 (C=O), 1610, 1588, 1559; HRMS (ESI) $^+$: m/z calcd for $[\text{C}_{19}\text{H}_{18}\text{N}_2\text{O}_3 + \text{Na}]^+$, 345.1210; observed, 345.1195.

Ethyl 1-(3-(3-(((1H-Pyrazole-4-carboxyl)oxy)methyl)-5-methoxyphenyl)prop-2-yn-1-yl)-1H-pyrazole-4-carboxylate (12). TFA (1 mL) was added to 3-(3-(4-(ethoxycarbonyl)-1H-pyrazol-1-yl)prop-1-yn-1-yl)-5-methoxybenzyl 1-(tetrahydro-2H-pyran-2-yl)-1H-pyrazole-4-carboxylate **46** (75 mg, 0.15 mmol). The reaction mixture was stirred over 15 min, then diluted with NaHCO_3 solution (20 mL) at 0 $^\circ\text{C}$, and extracted into DCM (3 \times 20 mL). The combined organic extracts were washed (brine), dried (MgSO_4), and concentrated in vacuo. Purification by flash column chromatography (0–100% ethyl acetate in petroleum ether) afforded **12** (42 mg, 63% yield). LCMS (ESI) $^+$: m/z 409.3 $[\text{M} + \text{H}]^+$, (ESI) $^-$: m/z 407.2 $[\text{M} - \text{H}]^-$, rt 1.89 min, >99%; ^1H NMR: (500 MHz, CDCl_3) 8.19 (1H, s), 8.10 (2H, s), 7.95 (1H, d, $J = 0.5$ Hz), 7.15–7.11 (1H, m), 6.98–6.94 (2H, m), 5.24 (2H, s), 5.17 (2H, s), 4.31 (2H, q, $J = 7.2$ Hz), 3.81 (2H, s), 1.35 (3H, t, $J = 7.2$ Hz); ^{13}C NMR: (125 MHz, CDCl_3) 163.1, 162.8, 159.7, 141.7, 138.2, 137.0 (br), 132.4, 124.0, 123.0, 116.5, 115.8, 115.4, 114.8, 86.9, 81.0, 65.3, 60.5, 55.6, 43.0, 14.5; $\nu_{\text{max}}/\text{cm}^{-1}$: 3127, 2977, 1706 (C=O), 1592, 1555; HRMS (ESI) $^+$: m/z calcd for $[\text{C}_{21}\text{H}_{20}\text{N}_4\text{O}_5 + \text{H}]^+$, 409.1506; observed, 409.1519.

3-Methoxy-5-(pyrrolidin-1-yl)benzyl 1H-Pyrazole-4-carboxylate (13). Pyrrolidine (0.110 mL, 1.32 mmol) and *tert*-butanol (2 mL) were added to a mixture of 3-bromo-5-methoxybenzyl 1-(tetrahydro-2H-pyran-2-yl)-1H-pyrazole-4-carboxylate **44** (0.500 g, 1.10 mmol), caesium carbonate (0.430 g, 1.32 mmol), RuPhos (26 mg, 0.055 mmol), and RuPhos Pd G1 methyl *tert*-butyl ether adduct (45 mg, 0.055 mmol). The reaction mixture was stirred at 85 $^\circ\text{C}$ over 15 h, then diluted with ethyl acetate (25 mL), washed with water (15 mL) and brine (15 mL), dried (MgSO_4), and concentrated in vacuo. TFA (4 mL) was added to the crude residue, and the reaction mixture was stirred over 30 min. The reaction mixture was diluted with ethyl acetate (100 mL), washed with NaHCO_3 solution (3 \times 100 mL) and brine (100 mL), dried (MgSO_4), and concentrated in vacuo. Purification by reverse phase chromatography (0–45% acetonitrile in water (+0.1% NH_3)), followed by flash column chromatography (0–4% methanol in DCM), afforded **13** (23 mg, 7% yield). LCMS (ESI) $^+$: m/z 302.2 $[\text{M} + \text{H}]^+$, (ESI) $^-$: m/z 300.1 $[\text{M} - \text{H}]^-$, rt 1.91 min, >99%; ^1H NMR: (500 MHz, CDCl_3) 8.09 (2H, s), 6.31–6.28 (1H, m), 6.25–6.22 (1H, m), 6.07 (1H, t, $J = 2.2$ Hz), 5.22 (2H, s), 3.80 (3H, s), 3.31–3.25 (4H, m), 2.02–1.96 (4H, m); ^{13}C NMR: (125 MHz, CDCl_3) 163.1, 161.0, 149.4, 138.0, 136.8, 115.1, 104.8, 100.7, 97.6, 66.9, 55.3, 47.8, 25.6; $\nu_{\text{max}}/\text{cm}^{-1}$: 3200 (br, N–H), 2962, 2840, 1712 (C=O), 1586; HRMS (ESI) $^+$: m/z calcd for $[\text{C}_{16}\text{H}_{19}\text{N}_3\text{O}_3 + \text{H}]^+$, 302.1499; observed, 302.1500.

3-Methoxy-5-(pyridin-3-yl)benzyl 1H-Pyrazole-4-carboxylate (14). Dioxane (2 mL) and water (0.5 mL) were added to a mixture of 3-bromo-5-methoxybenzyl 1-(tetrahydro-2H-pyran-2-yl)-1H-pyrazole-4-carboxylate **44** (0.200 g, 0.435 mmol), 3-pyridinylboronic acid (59 mg, 0.479 mmol), Pd(dppf) Cl_2 (16 mg, 0.022 mmol), and potassium carbonate (0.241 g, 1.74 mmol). The reaction mixture was heated to 100 $^\circ\text{C}$ by microwave for 30 min, then diluted with DCM (25 mL), washed with NaHCO_3 solution (3 \times 25 mL), dried (MgSO_4), and concentrated in vacuo. TFA (2 mL) was added to the crude residue, and the reaction mixture was stirred over 15 min. The reaction mixture was diluted with DCM (100 mL), washed with NaHCO_3 solution (3 \times 100 mL) and brine (100 mL), dried (MgSO_4), and concentrated in vacuo. Purification by flash column chromatography (75% ethyl acetate in petroleum ether) afforded **14** (59 mg, 44% yield). LCMS (ESI) $^+$: m/z 310.2 $[\text{M} + \text{H}]^+$, (ESI) $^-$: m/z 308.1 $[\text{M} - \text{H}]^-$, rt 1.45 min, >99%; ^1H NMR: (500 MHz, CD_3OD) 8.79 (1H, dd, $J = 2.3, 0.7$ Hz), 8.52 (1H, dd, $J = 5.0, 1.5$ Hz), 8.32–7.90 (2H, br s), 8.09 (1H, ddd, $J = 8.0, 2.3, 1.6$

Hz), 7.52 (1H, ddd, $J = 8.0, 4.9, 0.8$ Hz), 7.31–7.27 (1H, m), 7.16 (1H, t, $J = 2.0$ Hz), 7.10–7.04 (1H, m), 5.34 (2H, s), 3.87 (3H, s); ^{13}C NMR: (125 MHz, CD_3OD) 164.6, 162.1, 148.9, 148.3, 140.4, 140.3, 138.3, 136.8, 133.6 (br), 125.5, 120.1, 115.3, 114.6, 113.5, 66.7, 56.0; $\nu_{\text{max}}/\text{cm}^{-1}$: 3100 (br, N–H), 2940, 1708 (C=O), 1598, 1562; HRMS (ESI) $^+$: m/z calcd for $[\text{C}_{17}\text{H}_{15}\text{N}_3\text{O}_3 + \text{H}]^+$, 310.1186; observed, 310.1186.

3-Methoxy-5-(pyridin-3-ylmethyl)benzyl-1H-pyrazole-4-carboxylate (15). 1,2-Dimethoxyethane (4 mL) and water (1 mL) were added to a mixture of 3-methoxy-5-(4,4,5,5-tetramethyl-1,3,2-dioxaborolan-2-yl)benzyl 1-(tetrahydro-2H-pyran-2-yl)-1H-pyrazole-4-carboxylate **47** (0.192 g, 0.347 mmol), 3-(bromomethyl)pyridine hydrobromide (0.105 g, 0.417 mmol), tetrakis(triphenylphosphine)palladium(0) (40 mg, 0.035 mmol), and potassium carbonate (0.240 g, 1.74 mmol). The reaction mixture was heated to 95 °C over 10 h, then diluted with water (15 mL), and extracted into DCM (3 × 25 mL). The combined organic extracts were washed (brine), dried (MgSO_4), and concentrated in vacuo. Purification by flash column chromatography (0–100% ethyl acetate in petroleum ether) was attempted, and TFA (0.5 mL) was added to the resultant residue. The reaction mixture was stirred over 30 min, then diluted with NaHCO_3 solution (15 mL), and extracted into DCM (3 × 25 mL). The combined organic extracts were washed with NaHCO_3 solution (25 mL) and brine (25 mL), dried (MgSO_4), and concentrated in vacuo. Purification by flash column chromatography (0–100% ethyl acetate in petroleum ether, 0–10% methanol in DCM) afforded **15** (20 mg, 18% yield).

LCMS (ESI) $^+$: m/z 324.2 $[\text{M} + \text{H}]^+$, (ESI) $^-$: m/z 322.1 $[\text{M} - \text{H}]^-$, rt 1.30 min, 98%; ^1H NMR: (500 MHz, CDCl_3) 8.51 (1H, s), 8.47 (1H, d, $J = 4.9$ Hz), 8.06 (2H, s), 7.52–7.47 (1H, m), 7.22 (1H, dd, $J = 7.8, 4.9$ Hz), 6.84–6.79 (2H, m), 6.70–6.66 (1H, m), 5.23 (2H, s), 3.96 (2H, s), 3.78 (3H, s); ^{13}C NMR: (125 MHz, CDCl_3) 162.9, 160.2, 150.2, 147.8, 141.8, 138.1, 136.9, 136.7, 136.3, 123.7, 120.9, 114.9, 114.6, 111.7, 65.9, 55.5, 39.1; $\nu_{\text{max}}/\text{cm}^{-1}$: 3150 (br, N–H), 2936, 1709 (C=O), 1597, 1562; HRMS (ESI) $^+$: m/z calcd for $[\text{C}_{18}\text{H}_{17}\text{N}_3\text{O}_3 + \text{H}]^+$, 324.1343; observed, 324.1330.

5-(3-Methoxyphenyl)-1H-pyrazol-3-amine (19).²⁵ Hydrazine monohydrate (1.1 mL, 23 mmol) was added to a suspension of 3-(3-methoxyphenyl)-3-oxopropanenitrile **49** (0.400 g, 2.28 mmol) in ethanol (10 mL). The reaction mixture was heated under reflux for 6 h, then quenched with excess acetone at room temperature, and concentrated in vacuo. Purification by flash column chromatography (0–50% ethyl acetate in petroleum ether, 0–6% methanol in DCM) afforded **19** (0.314 g, 73% yield). LCMS (ESI) $^+$: m/z 190.2 $[\text{M} + \text{H}]^+$, rt 1.21 min, >99%; ^1H NMR: (500 MHz, CDCl_3) 7.28 (1H, t, $J = 8.0$ Hz), 7.13 (1H, dt, $J = 7.7, 1.2$ Hz), 7.09 (1H, t, $J = 2.0$ Hz), 6.86 (1H, ddd, $J = 8.2, 2.6, 0.8$ Hz), 5.89 (1H, s), 3.80 (3H, s); ^{13}C NMR: (125 MHz, CDCl_3) 160.1, 154.5, 145.7, 131.8, 130.1, 118.0, 114.0, 111.2, 90.7, 55.4; $\nu_{\text{max}}/\text{cm}^{-1}$: 3200 (br, N–H), 2837, 1612, 1589, 1567, 1506; HRMS (ESI) $^+$: m/z calcd for $[\text{C}_{10}\text{H}_{11}\text{N}_3\text{O} + \text{H}]^+$, 190.0975; observed, 190.0972.

5-(1-(4-Methoxybenzyl)-1H-indol-6-yl)-1H-pyrazol-3-amine (24a). Hydrazine monohydrate (42 μL , 0.67 mmol) was added to a solution of 3-(1-(4-methoxybenzyl)-1H-indol-6-yl)-3-oxopropanenitrile **55a** (0.200 g, 0.611 mmol) in ethanol (5 mL). The reaction mixture was heated under reflux for 30 min, and then further hydrazine monohydrate (0.114 mL, 1.83 mmol) was added at room temperature. The reaction mixture was heated under reflux for 4 h, then quenched with excess acetone at room temperature, and concentrated in vacuo. Purification by flash column chromatography (0–10% methanol in DCM) afforded **24a** (0.120 g, 62% yield). LCMS (ESI) $^+$: m/z 319.3 $[\text{M} + \text{H}]^+$, rt 1.65 min, >99%; ^1H NMR: (500 MHz, CDCl_3) 7.63 (1H, d, $J = 8.3$ Hz), 7.46 (1H, s), 7.30–7.25 (1H, m), 7.12 (1H, d, $J = 3.1$ Hz), 7.06–7.02 (2H, m), 6.83–6.78 (2H, m), 6.52 (1H, d, $J = 3.0$ Hz), 5.88 (1H, s), 5.22 (2H, s), 3.74 (3H, s); ^{13}C NMR: (125 MHz, CDCl_3) 159.3, 155.0, 146.7, 136.5, 129.5, 129.3, 129.1, 128.3, 123.8, 121.6, 117.7, 114.3, 106.8, 101.9, 90.5, 55.4, 49.7; $\nu_{\text{max}}/\text{cm}^{-1}$: 3150 (br, N–H), 2927, 1610, 1585, 1510; HRMS (ESI) $^+$: m/z calcd for $[\text{C}_{19}\text{H}_{18}\text{N}_4\text{O} + \text{H}]^+$, 319.1553; observed, 319.1557.

5-(1-(3-Methoxybenzyl)-1H-indol-6-yl)-1H-pyrazol-3-amine (24b). Hydrazine monohydrate (0.104 mL, 2.14 mmol) was added to a

solution of 3-(1-(3-methoxybenzyl)-1H-indol-6-yl)-3-oxopropanenitrile **55b** (65 mg, 0.21 mmol) in ethanol (4 mL). The reaction mixture was heated under reflux for 5 h and then concentrated in vacuo. Purification by flash column chromatography (0–100% ethyl acetate in petroleum ether, 0–10% methanol in DCM) was carried out, followed by reverse phase chromatography [0–40% acetonitrile in water (+0.1% formic acid)] with addition of NaHCO_3 solution (10 mL) to the combined fractions and extraction into DCM (3 × 25 mL). The combined organic extracts were washed (brine), dried (MgSO_4), and concentrated in vacuo to afford **24b** (27 mg, 40% yield). LCMS (ESI) $^+$: m/z 319.2 $[\text{M} + \text{H}]^+$, rt 1.65 min, >99%; ^1H NMR: (500 MHz, CDCl_3) 7.66 (1H, d, $J = 8.3$ Hz), 7.42 (1H, s), 7.29–7.25 (1H, m), 7.21 (1H, t, $J = 7.9$ Hz), 7.17 (1H, d, $J = 3.2$ Hz), 6.80 (1H, dd, $J = 8.2, 2.4$ Hz), 6.69 (1H, d, $J = 7.6$ Hz), 6.66–6.63 (1H, m), 6.56 (1H, dd, $J = 3.2, 0.7$ Hz), 5.89 (1H, s), 5.30 (2H, s), 3.72 (3H, s); ^{13}C NMR: (125 MHz, CDCl_3) 160.2, 155.2, 146.6, 138.9, 136.6, 130.1, 129.8, 129.2, 123.8, 121.7, 119.1, 117.7, 113.0, 112.8, 106.8, 102.1, 90.7, 55.3, 50.2; $\nu_{\text{max}}/\text{cm}^{-1}$: 3150 (br, N–H), 1585, 1505; HRMS (ESI) $^+$: m/z calcd for $[\text{C}_{19}\text{H}_{18}\text{N}_4\text{O} + \text{H}]^+$, 319.1553; observed, 319.1542.

5-(1-Benzyl-1H-indol-6-yl)-1H-pyrazol-3-amine (24c). Hydrazine monohydrate (0.271 mL, 5.58 mmol) was added to a solution of 3-(1-benzyl-1H-indol-6-yl)-3-oxopropanenitrile **55c** (0.170 g, 0.558 mmol) in ethanol (10 mL). The reaction mixture was heated under reflux for 8 h, then quenched with excess acetone at room temperature, and concentrated in vacuo. Purification by flash column chromatography (0–10% methanol in DCM) afforded **24c** (50 mg, 31% yield). LCMS (ESI) $^+$: m/z 289.3 $[\text{M} + \text{H}]^+$, rt 1.65 min, >99%; ^1H NMR: (400 MHz, CD_3OD) 7.63 (1H, s), 7.58 (1H, d, $J = 8.3$ Hz), 7.34 (1H, dd, $J = 8.4, 1.5$ Hz), 7.31–7.20 (4H, m), 7.16 (2H, d, $J = 7.2$ Hz), 6.50 (1H, d, $J = 3.1$ Hz), 5.90 (1H, s), 5.42 (2H, s); ^{13}C NMR: (125 MHz, CD_3OD) 155.6, 148.7, 139.5, 137.9, 130.7, 130.4, 129.7, 128.5, 127.9, 125.5, 122.0, 118.5, 107.7, 102.6, 90.2, 50.7; $\nu_{\text{max}}/\text{cm}^{-1}$: 2920, 2849, 1583, 1503; HRMS (ESI) $^+$: m/z calcd for $[\text{C}_{18}\text{H}_{16}\text{N}_4 + \text{H}]^+$, 289.1448; observed, 289.1446.

2-((6-(3-Amino-1H-pyrazol-5-yl)-1H-indol-1-yl)methyl)benzonitrile (24d). *n*-Butyllithium (1.6 M in hexanes, 4.09 mL, 6.54 mmol) was added dropwise at –78 °C to a mixture of acetonitrile (0.68 mL, 13 mmol) and toluene (5 mL). The reaction mixture was stirred at –78 °C over 30 min. A solution of methyl 1-(2-cyanobenzyl)-1H-indole-6-carboxylate **54d** (0.380 g, 1.31 mmol) in toluene (5 mL) was added dropwise at –78 °C over 30 min. The reaction mixture was stirred at –78 °C over 1 h, and then aqueous HCl (1 M, 15 mL) was added dropwise at 0 °C. The product was extracted into ethyl acetate (3 × 25 mL). The combined organic extracts were washed (brine), dried (MgSO_4), and concentrated in vacuo. Purification by flash column chromatography (0–80% ethyl acetate in petroleum ether) was attempted. Ethanol (20 mL) was added to the crude residue, followed by hydrazine monohydrate (0.50 mL, 10 mmol). The reaction mixture was heated under reflux for 5 h, then quenched with excess acetone at room temperature, and concentrated in vacuo. Purification by flash column chromatography (0–10% methanol in DCM) afforded **24d** (73 mg, 18% yield), with 14 mg subjected to further purification by flash column chromatography (0–100% ethyl acetate in petroleum ether, 0–5% methanol in DCM). LCMS (ESI) $^+$: m/z 314.3 $[\text{M} + \text{H}]^+$, rt 1.58 min, 96%; ^1H NMR: (400 MHz, CD_3OD) 7.77 (1H, dd, $J = 7.6, 1.1$ Hz), 7.63 (1H, s), 7.61 (1H, d, $J = 8.4$ Hz), 7.49 (1H, td, $J = 7.7, 1.2$ Hz), 7.44–7.35 (2H, m), 7.34 (1H, d, $J = 3.2$ Hz), 6.90 (1H, d, $J = 7.9$ Hz), 6.56 (1H, d, $J = 3.2$ Hz), 5.92 (1H, s), 5.64 (2H, s); ^{13}C NMR: (125 MHz, CD_3OD) 155.5, 148.5, 142.9, 137.9, 134.6, 134.2, 130.8, 130.4, 129.4, 128.8, 126.0, 122.2, 118.8, 118.3, 112.0, 107.5, 103.3, 90.2 (1 peak missing); $\nu_{\text{max}}/\text{cm}^{-1}$: 3200 (br, N–H), 2225 (C≡N), 1585, 1505; HRMS (ESI) $^+$: m/z calcd for $[\text{C}_{19}\text{H}_{15}\text{N}_5 + \text{H}]^+$, 314.1400; observed, 314.1402.

2-((6-(3-Amino-1H-pyrazol-5-yl)-1H-indol-1-yl)methyl)benzamide (24e). A suspension of 2-((6-(3-amino-1H-pyrazol-5-yl)-1H-indol-1-yl)methyl)benzonitrile **24d** (50 mg, 0.16 mmol) in aqueous NaOH (10 M, 4 mL) was heated under reflux for 7 h. The reaction mixture was adjusted to pH 3 and extracted into DCM/methanol (10:1, 3 × 75 mL). The combined organic extracts were washed (brine), dried (MgSO_4), and concentrated in vacuo.

Purification by reverse phase column chromatography (0–35% acetonitrile in water) afforded **24e** (15 mg, 28% yield). LCMS (ESI⁺): m/z 332.3 [M + H]⁺, (ESI⁻): m/z 330.1 [M - H]⁻, rt 1.47 min, >99%; ¹H NMR: (500 MHz, CD₃OD) 7.62–7.52 (3H, m), 7.37–7.24 (4H, m), 6.82–6.75 (1H, m), 6.51 (1H, d, J = 3.0 Hz), 5.90 (1H, s), 5.64 (2H, s); ¹³C NMR: (125 MHz, CD₃OD) 174.6, 138.0, 137.7, 135.9, 131.6, 131.2, 130.3, 128.7, 128.5, 125.3 (br), 122.0, 118.5, 107.7, 102.7, 90.5 (br), 48.3 (3 peaks missing); $\nu_{\max}/\text{cm}^{-1}$: 3200 (br), 1635 (C=O), 1505; HRMS (ESI⁺): m/z calcd for [C₁₉H₁₇N₅O + H]⁺, 332.1506; observed, 332.1504.

3-Amino-5-(1H-indol-6-yl)-1H-pyrazole-4-carbonitrile (25). Hydrazine monohydrate (0.163 mL, 3.36 mmol) was added to a suspension of 3-amino-4,4,4-trichloro-2-(1H-indole-6-carbonyl)but-2-enenitrile **53** (0.690 g, 2.10 mmol) in ethanol (10 mL). The reaction mixture was heated under reflux for 22 h and then quenched with excess acetone at room temperature and concentrated in vacuo. Purification by flash column chromatography (0–100% ethyl acetate in petroleum ether) afforded **25** (0.113 g, 24% yield). LCMS (ESI⁺): m/z 224.2 [M + H]⁺, (ESI⁻): m/z 222.1 [M - H]⁻, rt 1.50 min, >99%; ¹H NMR: (400 MHz, CD₃OD) 7.89 (1H, s), 7.63 (1H, d, J = 8.0 Hz), 7.45 (1H, d, J = 7.0 Hz), 7.33 (1H, d, J = 2.1 Hz), 6.50 (1H, d, J = 2.7 Hz); ¹³C NMR: (125 MHz, CD₃OD) 137.5, 130.6, 127.8, 121.7, 118.5, 116.9, 110.6, 102.6 (4 peaks missing); $\nu_{\max}/\text{cm}^{-1}$: 3411 (N-H), 3200 (br, N-H), 2221 (C≡N), 1634, 1584, 1527; HRMS (ESI⁺): m/z calcd for [C₁₂H₉N₅ + H]⁺, 224.0931; observed, 224.0935.

3-Amino-5-(1-Benzyl-1H-indol-6-yl)-1H-pyrazole-4-carbonitrile (26c). Trichloroacetonitrile (0.168 mL, 1.67 mmol) was added to a suspension of 3-(1-benzyl-1H-indol-6-yl)-3-oxopropanenitrile **55c** (0.170 g, 0.558 mmol) and sodium acetate (0.229 g, 2.79 mmol) in ethanol (5 mL). The reaction mixture was stirred over 9 h, then concentrated in vacuo, diluted with water (20 mL), and extracted into DCM (3 × 25 mL). The combined organic extracts were washed (brine), dried (MgSO₄), and concentrated in vacuo. The crude residue was dissolved in ethanol (10 mL), and hydrazine monohydrate (0.271 mL, 5.58 mmol) was added. The reaction mixture was heated under reflux for 5 h, then quenched with excess acetone at room temperature, and concentrated in vacuo. Purification by flash column chromatography (0–100% ethyl acetate in petroleum ether) afforded **26c** (78 mg, 45% yield). LCMS (ESI⁺): m/z 314.2 [M + H]⁺, (ESI⁻): m/z 312.1 [M - H]⁻, rt 1.84 min, 100%; ¹H NMR: (500 MHz, CDCl₃) 7.72 (1H, s), 7.67 (1H, d, J = 8.3 Hz), 7.41 (1H, dd, J = 8.2, 1.5 Hz), 7.29–7.19 (4H, m), 7.13–7.08 (2H, m), 6.57 (1H, dd, J = 3.1, 0.8 Hz), 5.26 (2H, s), 4.12 (2H, br s); ¹³C NMR: (125 MHz, CDCl₃) 157.0, 150.1, 136.9, 136.2, 130.8, 130.4, 129.0, 128.0, 127.1, 122.0, 120.8, 117.6, 115.3, 108.2, 102.3, 76.1, 50.4; $\nu_{\max}/\text{cm}^{-1}$: 3200 (br, N-H), 2211 (C≡N), 1621, 1582, 1524, 1501; HRMS (ESI⁺): m/z calcd for [C₁₉H₁₅N₅ + H]⁺, 314.1400; observed, 314.1404.

3-Amino-5-(1-(pyridin-3-ylmethyl)-1H-indol-6-yl)-1H-pyrazole-4-carbonitrile (26g). Trichloroacetonitrile (0.647 mL, 6.45 mmol) was added to a suspension of 3-oxo-3-(1-(pyridin-3-ylmethyl)-1H-indol-6-yl)propanenitrile **55g** (0.592 g, 2.15 mmol) and sodium acetate (0.882 g, 10.8 mmol) in ethanol (20 mL). The reaction mixture was stirred over 13 h, then concentrated in vacuo, diluted with water (20 mL), and extracted into DCM (3 × 25 mL). The combined organic extracts were washed (brine), dried (MgSO₄), and concentrated in vacuo. The crude residue was dissolved in ethanol (20 mL), and hydrazine monohydrate (1.1 mL, 22 mmol) was added. The reaction mixture was heated under reflux for 21 h, then quenched with excess acetone at room temperature, and concentrated in vacuo. Purification by flash column chromatography (0–100% ethyl acetate in DCM, 5% methanol in DCM) afforded **26g** (0.367 g, 54% yield). LCMS (ESI⁺): m/z 315.2 [M + H]⁺, (ESI⁻): m/z 313.1 [M - H]⁻, rt 1.38 min, >99%; ¹H NMR: (400 MHz, (CD₃)₂SO) 12.09 (1H, br s), 8.56 (1H, s), 8.46 (1H, dd, J = 4.7, 1.3 Hz), 7.90 (1H, s), 7.74–7.56 (3H, m), 7.50 (1H, d, J = 8.2 Hz), 7.32 (1H, dd, J = 7.7, 4.8 Hz), 6.55 (1H, d, J = 2.8 Hz), 6.26 (2H, br s), 5.49 (2H, s); ¹³C NMR: (100 MHz, (CD₃)₂SO) 148.8, 148.5, 135.4, 135.0, 133.5, 130.6, 128.9, 123.7, 120.9, 117.5, 116.5, 107.4, 101.6, 46.8 (4 peaks missing); $\nu_{\max}/\text{cm}^{-1}$: 3345 (N-H), 3100 (br, N-H), 2215 (C≡N), 1662, 1600, 1502; HRMS (ESI⁺): m/z calcd for [C₁₈H₁₄N₆ - H]⁻, 313.1207; observed, 313.1195.

3-Amino-5-(1-((2-hydroxypyridin-3-yl)methyl)-1H-indol-6-yl)-1H-pyrazole-4-carbonitrile (26j). Lithium chloride (12 mg, 0.29 mmol) and *p*-toluenesulfonic acid monohydrate (55 mg, 0.29 mmol) were added to a solution of 3-amino-5-(1-((2-methoxypyridin-3-yl)methyl)-1H-indol-6-yl)-1H-pyrazole-4-carbonitrile **26h** (20 mg, 0.058 mmol) in DMF (1 mL). The reaction mixture was heated to 120 °C over 25 min, then diluted with ethyl acetate (100 mL), washed with water (3 × 100 mL) and brine (100 mL), dried (MgSO₄), and concentrated in vacuo. Purification by flash column chromatography (50–100% ethyl acetate in petroleum ether, 0–10% methanol in DCM) afforded **26j** (10 mg, 51% yield). LCMS (ESI⁺): m/z 331.2 [M + H]⁺, (ESI⁻): m/z 329.1 [M - H]⁻, rt 1.55 min, 97%; ¹H NMR: (500 MHz, CD₃OD) 7.82 (1H, s), 7.66 (1H, d, J = 8.1 Hz), 7.51 (1H, d, J = 7.5 Hz), 7.45 (1H, s), 7.32 (1H, dd, J = 6.5, 2.0 Hz), 7.08 (1H, d, J = 4.8 Hz), 6.55 (1H, d, J = 2.8 Hz), 6.25 (1H, t, J = 6.7 Hz), 5.28 (2H, s); ¹³C NMR: (125 MHz, CD₃OD) 164.1, 140.1, 137.4, 135.0, 132.1, 131.4, 129.6, 122.3, 119.0, 116.9, 109.0, 108.0, 102.7, 46.2 (4 peaks missing); $\nu_{\max}/\text{cm}^{-1}$: 3150 (br, N-H/O-H), 2925, 2207 (C≡N), 1647, 1611, 1564, 1529, 1501; HRMS (ESI⁺): m/z calcd for [C₁₈H₁₄N₆O + Na]⁺, 353.1121; observed, 353.1105.

3-Amino-5-(1-((6-hydroxypyridin-3-yl)methyl)-1H-indol-6-yl)-1H-pyrazole-4-carbonitrile (26k). Lithium chloride (26 mg, 0.61 mmol) and *p*-toluenesulfonic acid monohydrate (0.116 g, 0.610 mmol) were added to a solution of 3-amino-5-(1-((6-methoxypyridin-3-yl)methyl)-1H-indol-6-yl)-1H-pyrazole-4-carbonitrile **26i** (42 mg, 0.12 mmol) in DMF (1 mL). The reaction mixture was heated to 120 °C over 25 min, then diluted with ethyl acetate (100 mL), washed with water (3 × 100 mL) and brine (100 mL), dried (MgSO₄), and concentrated in vacuo. Purification by flash column chromatography (50–100% ethyl acetate in petroleum ether, 0–12% methanol in DCM) afforded **26k** (19 mg, 47% yield). LCMS (ESI⁺): m/z 331.2 [M + H]⁺, (ESI⁻): m/z 329.1 [M - H]⁻, rt 1.47 min, >99%; ¹H NMR: (500 MHz, (CD₃)₂SO) 12.01 (1H, br s), 11.54 (1H, br s), 7.94 (1H, s), 7.73–7.29 (5H, m), 6.51 (1H, d, J = 2.4 Hz), 6.39 (1H, br s), 6.26 (1H, d, J = 9.3 Hz), 5.15 (2H, s); ¹³C NMR: (125 MHz, (CD₃)₂SO) 161.9, 141.0, 135.3, 133.9, 130.3, 128.8, 125.6, 120.8, 120.3, 117.4, 116.6, 114.6, 107.5, 101.4, 45.7 (3 peaks missing); $\nu_{\max}/\text{cm}^{-1}$: 3436, 3340, 3231, 2941, 2211 (C≡N), 1661, 1614, 1533; HRMS (ESI⁺): m/z calcd for [C₁₈H₁₄N₆O + H]⁺, 331.1302; observed, 331.1289.

3-Amino-5-(1-(pyridin-4-ylmethyl)-1H-indol-6-yl)-1H-pyrazole-4-carbonitrile (26l). Trichloroacetonitrile (0.309 mL, 3.08 mmol) was added to a suspension of 3-oxo-3-(1-(pyridin-4-ylmethyl)-1H-indol-6-yl)propanenitrile **55l** (0.283 g, 1.03 mmol) and sodium acetate (0.422 g, 5.14 mmol) in ethanol (20 mL). The reaction mixture was stirred over 13 h, then concentrated in vacuo, diluted with water (20 mL), and extracted into DCM (4 × 25 mL). The combined organic extracts were washed (brine), dried (MgSO₄), and concentrated in vacuo. The crude residue was dissolved in ethanol (20 mL), and hydrazine monohydrate (0.500 mL, 10.3 mmol) was added. The reaction mixture was heated under reflux for 21 h, then quenched with excess acetone at room temperature, and concentrated in vacuo. Purification by flash column chromatography (0–100% ethyl acetate in DCM, 8% methanol in DCM) afforded **26l** (0.183 g, 57% yield). LCMS (ESI⁺): m/z 315.2 [M + H]⁺, (ESI⁻): m/z 313.1 [M - H]⁻, rt 1.35 min, >99%; ¹H NMR: (500 MHz, CD₃OD) 8.40–8.36 (2H, m), 7.73 (1H, s), 7.66 (1H, d, J = 8.3 Hz), 7.53 (1H, dd, J = 8.2, 1.1 Hz), 7.37 (1H, d, J = 3.2 Hz), 7.12–7.08 (2H, m), 6.58 (1H, dd, J = 3.2, 0.8 Hz), 5.43 (2H, s); ¹³C NMR: (125 MHz, CD₃OD) 157.8, 152.5, 150.3, 149.7, 137.4, 131.7, 131.3, 124.6, 123.3, 122.4, 119.2, 116.9, 108.8, 103.3, 73.9, 49.7; $\nu_{\max}/\text{cm}^{-1}$: 2204 (C≡N), 1605, 1554, 1500; HRMS (ESI⁺): m/z calcd for [C₁₈H₁₄N₆ + H]⁺, 315.1353; observed, 315.1350.

3-Amino-5-(1-(quinolin-4-ylmethyl)-1H-indol-6-yl)-1H-pyrazole-4-carbonitrile (26m). Trichloroacetonitrile (92 μL, 0.91 mmol) was added to a suspension of 3-oxo-3-(1-(quinolin-4-ylmethyl)-1H-indol-6-yl)propanenitrile **55m** (99 mg, 0.30 mmol) and sodium acetate (0.125 g, 1.52 mmol) in ethanol (10 mL). The reaction mixture was stirred over 36 h, then diluted with water (50 mL), and extracted into DCM (3 × 50 mL). The combined organic extracts were washed (brine), dried (MgSO₄), and concentrated in vacuo. The crude residue was dissolved in ethanol (10 mL), and hydrazine monohydrate (0.148

mL, 3.04 mmol) was added. The reaction mixture was heated under reflux for 6 h and then concentrated in vacuo. Purification by flash column chromatography (50–100% ethyl acetate in petroleum ether) afforded **26m** (45 mg, 41% yield). LCMS (ESI⁺): *m/z* 365.3 [M + H]⁺, (ESI⁻): *m/z* 363.2 [M - H]⁻, rt 1.55 min, >99%; ¹H NMR: (400 MHz, CD₃OD) 8.61 (1H, d, *J* = 4.6 Hz), 8.23 (1H, d, *J* = 8.3 Hz), 8.07 (1H, d, *J* = 8.6 Hz), 7.81 (1H, t, *J* = 7.9 Hz), 7.76–7.65 (3H, m), 7.57 (1H, d, *J* = 7.9 Hz), 7.41 (1H, s), 6.65 (1H, d, *J* = 2.9 Hz), 6.62 (1H, d, *J* = 4.6 Hz), 5.99 (2H, s); ¹³C NMR: (125 MHz, CD₃OD) 151.2, 148.5, 146.2, 137.8, 131.6, 131.2, 129.9, 128.6, 127.3, 124.3, 122.4, 119.6, 119.5, 117.0, 108.8, 103.6, 47.7 (5 peaks missing); $\nu_{\max}/\text{cm}^{-1}$: 3150 (br, N-H), 2210 (C≡N), 1621, 1595, 1504; HRMS (ESI⁺): *m/z* calcd for [C₂₂H₁₆N₆ + Na]⁺, 387.1329; observed, 387.1328.

3-Amino-5-(1-(1-methylpiperidin-2-yl)methyl)-1H-indol-6-yl)-1H-pyrazole-4-carbonitrile (26n). Trichloroacetonitrile (42 μ L, 0.42 mmol) was added to a suspension of 3-(1-(1-methylpiperidin-2-yl)methyl)-1H-indol-6-yl)-3-oxopropanenitrile **55n** (43 mg, 0.14 mmol) and sodium acetate (58 mg, 0.71 mmol) in ethanol (5 mL). The reaction mixture was stirred over 18 h, then diluted with NaHCO₃ solution (12.5 mL) and water (12.5 mL), and extracted into DCM (3 \times 25 mL). The combined organic extracts were washed (brine), dried (MgSO₄), and concentrated in vacuo. The crude residue was dissolved in ethanol (5 mL), and hydrazine monohydrate (69 μ L, 1.4 mmol) was added. The reaction mixture was heated under reflux for 24 h and then concentrated in vacuo. Purification by flash column chromatography (50–100% ethyl acetate in petroleum ether, 0–16% methanol in DCM) afforded **26n** (27 mg, 57% yield). LCMS (ESI⁺): *m/z* 335.3 [M + H]⁺, (ESI⁻): *m/z* 333.2 [M - H]⁻, rt 1.22 min, >99%; ¹H NMR: (500 MHz, CD₃OD) 7.90 (1H, s), 7.64 (1H, d, *J* = 8.4 Hz), 7.50 (1H, dd, *J* = 8.4, 0.9 Hz), 7.31 (1H, d, *J* = 3.2 Hz), 6.52 (1H, dd, *J* = 3.2, 0.6 Hz), 4.74 (1H, dd, *J* = 14.3, 4.7 Hz), 4.07 (1H, dd, *J* = 14.4, 9.5 Hz), 3.11–3.03 (1H, m), 2.97–2.87 (1H, m), 2.66 (3H, s), 2.51 (1H, td, *J* = 11.3, 3.4 Hz), 1.74–1.58 (3H, m), 1.41–1.18 (3H, m); ¹³C NMR: (125 MHz, CD₃OD) 157.9 (br), 152.8 (br), 137.5, 131.8, 131.3, 124.4 (br), 122.4, 119.0, 117.2, 109.1, 102.9, 74.3 (br), 64.2, 57.7, 42.8, 29.5, 25.5, 23.7 (1 peak missing); $\nu_{\max}/\text{cm}^{-1}$: 3150 (br, N-H), 2927, 2210 (C≡N), 1623, 1589, 1525, 1503; HRMS (ESI⁺): *m/z* calcd for [C₁₉H₂₂N₆ + H]⁺, 335.1979; observed, 335.1971.

3-Amino-5-(1-(1-methylpiperidin-3-yl)methyl)-1H-indol-6-yl)-1H-pyrazole-4-carbonitrile (26o). Trichloroacetonitrile (0.143 mL, 1.42 mmol) was added to a suspension of 3-(1-(1-methylpiperidin-3-yl)methyl)-1H-indol-6-yl)-3-oxopropanenitrile **55o** (0.140 g, 0.474 mmol) and sodium acetate (0.194 g, 2.37 mmol) in ethanol (3 mL). The reaction mixture was stirred over 3 h 30 min, then diluted with NaHCO₃ solution (10 mL), and extracted into DCM (3 \times 25 mL). The combined organic extracts were washed (brine), dried (MgSO₄), and concentrated in vacuo. The crude residue was dissolved in ethanol (5 mL), and hydrazine monohydrate (0.231 mL, 4.74 mmol) was added. The reaction mixture was heated under reflux for 15 h and then concentrated in vacuo. Purification by flash column chromatography (50–100% ethyl acetate in petroleum ether, 0–20% methanol in DCM) was carried out, followed by reverse phase chromatography (0–8% acetonitrile in water (+0.1% formic acid)) with addition of NaHCO₃ solution (40 mL) to the combined fractions and extraction into DCM/methanol (9:1, 4 \times 50 mL). The combined organic extracts were washed (brine), dried (MgSO₄), and concentrated in vacuo to afford **26o** (61 mg, 38% yield). LCMS (ESI⁺): *m/z* 335.3 [M + H]⁺, (ESI⁻): *m/z* 333.2 [M - H]⁻, rt 1.23 min, >99%; ¹H NMR: (500 MHz, CDCl₃) 7.78 (1H, s), 7.63 (1H, d, *J* = 8.3 Hz), 7.41 (1H, dd, *J* = 8.2, 1.4 Hz), 7.11 (1H, d, *J* = 3.2 Hz), 6.49 (1H, dd, *J* = 3.0, 0.6 Hz), 4.44 (2H, br s), 4.05–3.91 (2H, m), 2.68 (1H, d, *J* = 9.6 Hz), 2.61 (1H, d, *J* = 10.4 Hz), 2.32–2.21 (1H, m), 2.17 (3H, s), 2.05–1.88 (1H, m), 1.77 (1H, t, *J* = 10.2 Hz), 1.69–1.45 (3H, m), 1.06–0.92 (1H, m); ¹³C NMR: (125 MHz, CDCl₃) 157.1, 150.2, 136.2, 130.8, 130.1, 121.8, 121.1, 117.6, 115.7, 108.2, 101.7, 76.0, 59.4, 56.1, 50.4, 46.4, 37.0, 28.0, 24.5; $\nu_{\max}/\text{cm}^{-1}$: 3200 (br, N-H), 2932, 2788, 2209 (C≡N), 1622, 1590, 1524, 1501; HRMS (ESI⁺): *m/z* calcd for [C₁₉H₂₂N₆ + H]⁺, 335.1979; observed, 335.1983.

3-Amino-5-(3-chloro-1-(pyridin-3-ylmethyl)-1H-indol-6-yl)-1H-pyrazole-4-carbonitrile (27g). *N*-Chlorosuccinimide (21 mg,

0.16 mmol) was added to a solution of 3-amino-5-(1-(pyridin-3-ylmethyl)-1H-indol-6-yl)-1H-pyrazole-4-carbonitrile **26g** (50 mg, 0.16 mmol) in DMF (1 mL). The reaction mixture was stirred over 6 h, and then further *N*-chlorosuccinimide (7 mg, 0.05 mmol) was added. The reaction mixture was stirred over 90 min, then diluted with ethyl acetate (100 mL), washed with NaHCO₃ solution (2 \times 100 mL) and brine (100 mL), dried (MgSO₄), and concentrated in vacuo. Purification by flash column chromatography (0–100% ethyl acetate in petroleum ether, 0–7% methanol in DCM), followed by reverse phase column chromatography (0–50% acetonitrile in water), afforded **27g** (35 mg, 63% yield). LCMS (ESI⁺): *m/z* 349.2 [M + H]⁺, (ESI⁻): *m/z* 347.1 [M - H]⁻, rt 1.57 min, >99%; ¹H NMR: (500 MHz, (CD₃)₂SO) 8.60 (1H, d, *J* = 1.8 Hz), 8.47 (1H, dd, *J* = 4.8, 1.6 Hz), 7.97 (1H, s), 7.88 (1H, s), 7.67 (1H, dt, *J* = 7.9, 1.9 Hz), 7.61 (1H, dd, *J* = 8.4, 1.3 Hz), 7.58 (1H, d, *J* = 8.4 Hz), 7.33 (1H, ddd, *J* = 7.9, 4.7, 0.8 Hz), 6.22 (2H, br s), 5.48 (2H, s); ¹³C NMR: (125 MHz, (CD₃)₂SO) 155.7, 149.6, 149.0, 148.6, 135.1, 134.6, 133.0, 127.2, 126.0, 125.4, 123.8, 118.4, 118.0, 116.5, 108.0, 103.5, 70.8, 47.0; $\nu_{\max}/\text{cm}^{-1}$: 3344 (N-H), 2218 (C≡N), 1623, 1586, 1525; HRMS (ESI⁻): *m/z* calcd for [C₁₈H₁₃ClN₆ - H]⁻, 347.0817; observed, 347.0804.

3-Amino-5-(1-(4-(piperidin-1-ylmethyl)benzyl)-1H-indol-6-yl)-1H-pyrazole-4-carbonitrile (29b). Trichloroacetonitrile (0.138 mL, 1.37 mmol) was added to a suspension of 3-oxo-3-(1-(4-(piperidin-1-ylmethyl)benzyl)-1H-indol-6-yl)propanenitrile **83b** (0.170 g, 0.458 mmol) and sodium acetate (0.188 g, 2.29 mmol) in ethanol (5 mL). The reaction mixture was stirred over 44 h, then diluted with NaHCO₃ solution (10 mL) and water (10 mL), and extracted into DCM (3 \times 20 mL). The combined organic extracts were washed (brine), dried (MgSO₄), and concentrated in vacuo. The crude residue was dissolved in ethanol (10 mL), and hydrazine monohydrate (0.223 mL, 4.58 mmol) was added. The reaction mixture was heated under reflux for 24 h, then concentrated in vacuo. Purification by flash column chromatography (0–100% ethyl acetate in petroleum ether, 0–15% methanol in DCM) was carried out, followed by reverse phase chromatography (0–35% acetonitrile in water (+0.1% formic acid)) with adjustment of the combined fractions to pH 8 and extraction into DCM/methanol (10:1, 3 \times 50 mL). The combined organic extracts were washed (brine), dried (MgSO₄), and concentrated in vacuo to afford **29b** (60 mg, 32% yield). LCMS (ESI⁺): *m/z* 411.3 [M + H]⁺, rt 1.44 min, >99%; ¹H NMR: (500 MHz, CDCl₃) 7.70 (1H, s), 7.63 (1H, d, *J* = 8.2 Hz), 7.40 (1H, dd, *J* = 8.2, 1.4 Hz), 7.21 (2H, d, *J* = 8.1 Hz), 7.19 (1H, d, *J* = 3.1 Hz), 7.04 (2H, d, *J* = 7.9 Hz), 6.54 (1H, dd, *J* = 3.2, 0.6 Hz), 5.20 (2H, s), 4.33 (2H, br s), 3.42 (2H, s), 2.36 (4H, br s), 1.50 (4H, quin, *J* = 5.6 Hz), 1.42–1.33 (2H, m); ¹³C NMR: (125 MHz, CDCl₃) 156.8, 150.2, 137.4, 136.2, 136.0, 130.6, 130.21, 130.17, 127.1, 121.9, 121.4, 117.7, 115.7, 108.1, 102.2, 75.7, 63.3, 54.5, 50.1, 25.6, 24.2; $\nu_{\max}/\text{cm}^{-1}$: 3200 (br, N-H), 2931, 2211 (C≡N), 1621, 1584, 1502; HRMS (ESI⁺): *m/z* calcd for [C₂₅H₂₆N₆ + H]⁺, 411.2292; observed, 411.2287.

3-Amino-5-(1-(4-(morpholinomethyl)benzyl)-1H-indol-6-yl)-1H-pyrazole-4-carbonitrile (29c). Trichloroacetonitrile (0.142 mL, 1.42 mmol) was added to a suspension of 3-(1-(4-(morpholinomethyl)benzyl)-1H-indol-6-yl)-3-oxopropanenitrile **83c** (0.190 g, 0.473 mmol) and sodium acetate (0.194 g, 2.37 mmol) in ethanol (5 mL). The reaction mixture was stirred over 14 h, then diluted with NaHCO₃ solution (15 mL), and extracted into DCM (3 \times 25 mL). The combined organic extracts were washed (brine), dried (MgSO₄), and concentrated in vacuo. The crude residue was dissolved in ethanol (5 mL), and hydrazine monohydrate (0.230 mL, 4.73 mmol) was added. The reaction mixture was heated under reflux for 22 h and then concentrated in vacuo. Purification by flash column chromatography (0–100% ethyl acetate in petroleum ether, 0–10% methanol in DCM) was carried out, followed by reverse phase chromatography (100% water (+0.1% formic acid)) with adjustment of the combined fractions to pH 8 and extraction into DCM/methanol (10:1, 3 \times 50 mL). The combined organic extracts were washed (brine), dried (MgSO₄), and concentrated in vacuo to afford **29c** (81 mg, 42% yield). LCMS (ESI⁺): *m/z* 413.3 [M + H]⁺, rt 1.36 min, >99%; ¹H NMR: (500 MHz, CDCl₃) 7.73 (1H, s), 7.66 (1H, d, *J* = 8.2 Hz), 7.39 (1H, dd, *J* = 8.3, 1.3 Hz), 7.25–7.20 (3H, m), 7.08 (2H, d, *J* = 8.1 Hz), 6.56 (1H, dd,

$J = 3.2, 0.6$ Hz), 5.26 (2H, s), 4.20 (2H, s), 3.64 (4H, t, $J = 4.6$ Hz), 3.41 (2H, s), 2.47–2.31 (4H, m); ^{13}C NMR: (125 MHz, CDCl_3) 157.0, 150.1, 137.6, 136.2, 135.9, 130.7, 130.4, 129.9, 127.1, 122.0, 121.0, 117.6, 115.4, 108.2, 102.3, 76.1, 67.0, 63.1, 53.7, 50.2; $\nu_{\text{max}}/\text{cm}^{-1}$: 3200 (br, N–H), 2922, 2212 ($\text{C}\equiv\text{N}$), 1740, 1624, 1584, 1502; HRMS (ESI^+): m/z calcd for $[\text{C}_{24}\text{H}_{24}\text{N}_6\text{O} + \text{H}]^+$, 413.2084; observed, 413.2079.

3-Amino-5-(1-(4-((4-isopropylpiperazin-1-yl)methyl)benzyl)-1H-indol-6-yl)-1H-pyrazole-4-carbonitrile (29e). Trichloroacetonitrile (0.129 mL, 1.29 mmol) was added to a suspension of 3-(1-(4-((4-isopropylpiperazin-1-yl)methyl)benzyl)-1H-indol-6-yl)-3-oxopropanenitrile **83e** (0.178 g, 0.429 mmol) and sodium acetate (0.176 g, 2.15 mmol) in ethanol (5 mL). The reaction mixture was stirred over 10 h, then diluted with NaHCO_3 solution (7.5 mL) and water (7.5 mL), and extracted into DCM (3×25 mL). The combined organic extracts were washed (brine), dried (MgSO_4), and concentrated in vacuo. The crude residue was dissolved in ethanol (3 mL), and hydrazine monohydrate (0.209 mL, 4.29 mmol) was added. The reaction mixture was heated under reflux for 7 h, then quenched with excess acetone at room temperature, and concentrated in vacuo. Purification by flash column chromatography (50–100% ethyl acetate in petroleum ether, 0–20% methanol in DCM (+0.1% NH_3)) afforded **29e** (0.147 g, 75% yield). LCMS (ESI^+): m/z 454.3 $[\text{M} + \text{H}]^+$, (ESI^-): m/z 452.3 $[\text{M} - \text{H}]^-$, rt 1.40 min, >99%; ^1H NMR: (500 MHz, CD_3OD) 7.81 (1H, s), 7.63 (1H, d, $J = 8.3$ Hz), 7.48 (1H, d, $J = 8.1$ Hz), 7.39 (1H, d, $J = 2.6$ Hz), 7.25 (2H, d, $J = 8.1$ Hz), 7.21 (2H, d, $J = 8.2$ Hz), 6.53 (1H, d, $J = 3.2$ Hz), 5.36 (2H, s), 3.55 (2H, s), 3.36–3.29 (1H, m), 3.10 (4H, br s), 2.69 (4H, br s), 1.27 (6H, d, $J = 6.9$ Hz); ^{13}C NMR: (125 MHz, CD_3OD) 138.6, 137.3, 137.1, 131.6, 131.4, 130.8, 128.5, 122.2, 118.7, 117.0, 109.2, 102.7, 62.3, 59.0, 51.0, 50.8, 49.4, 17.3 (4 peaks missing); $\nu_{\text{max}}/\text{cm}^{-1}$: 2210 ($\text{C}\equiv\text{N}$), 1623, 1587, 1501; HRMS (ESI^+): m/z calcd for $[\text{C}_{27}\text{H}_{31}\text{N}_7 + \text{H}]^+$, 454.2714; observed, 454.2715.

4-Methyl-5-(1-(4-(pyrrolidin-1-ylmethyl)benzyl)-1H-indol-6-yl)-1H-pyrazol-3-amine (30a). Hydrazine monohydrate (0.147 mL, 3.01 mmol) was added to a solution of 2-methyl-3-oxo-3-(1-(4-(pyrrolidin-1-ylmethyl)benzyl)-1H-indol-6-yl)propanenitrile **84a** (0.140 g, 0.301 mmol) in ethanol (5 mL). The reaction mixture was heated under reflux for 28 h, then quenched with excess acetone at room temperature, and concentrated in vacuo. Purification by flash column chromatography [50–100% ethyl acetate in petroleum ether, 0–20% methanol (+0.1% NH_3)] afforded **30a** (24 mg, 21% yield). LCMS (ESI^+): m/z 386.3 $[\text{M} + \text{H}]^+$, rt 1.25 min, >99%; ^1H NMR: (500 MHz, CDCl_3) 7.69 (1H, d, $J = 8.2$ Hz), 7.30 (1H, s), 7.26 (2H, d, $J = 8.1$ Hz), 7.20 (1H, d, $J = 3.2$ Hz), 7.18 (1H, dd, $J = 8.4, 1.5$ Hz), 7.08 (2H, d, $J = 8.1$ Hz), 6.57 (1H, dd, $J = 3.1, 0.7$ Hz), 5.31 (2H, s), 3.58 (2H, s), 2.53–2.43 (4H, m), 1.98 (3H, s), 1.81–1.71 (4H, m); ^{13}C NMR: (125 MHz, CDCl_3) 154.4, 142.7, 139.1, 136.4, 135.8, 129.7, 129.6, 128.8, 126.9, 124.3, 121.5, 119.0, 108.8, 101.9, 99.3, 60.3, 54.2, 50.3, 23.5, 7.9; $\nu_{\text{max}}/\text{cm}^{-1}$: 3200 (br, N–H), 2916, 2788, 1606, 1502; HRMS (ESI^+): m/z calcd for $[\text{C}_{24}\text{H}_{27}\text{N}_5 + \text{H}]^+$, 386.2339; observed, 386.2354.

5-(1-(4-(Piperidin-1-ylmethyl)benzyl)-1H-indol-6-yl)-1H-pyrazol-3-amine (31b). Hydrazine monohydrate (0.136 mL, 2.80 mmol) was added to a solution of 3-oxo-3-(1-(4-(piperidin-1-ylmethyl)benzyl)-1H-indol-6-yl)propanenitrile **83b** (0.104 g, 0.280 mmol) in ethanol (5 mL). The reaction mixture was heated under reflux for 21 h and then concentrated in vacuo. Purification by flash column chromatography (0–100% ethyl acetate in petroleum ether, 0–15% methanol in DCM) was carried out, followed by reverse phase chromatography [0–20% acetonitrile in water (+0.1% formic acid)] with adjustment of the combined fractions to pH 14 and extraction into DCM (3×25 mL). The combined organic extracts were washed (brine), dried (MgSO_4), and concentrated in vacuo to afford **31b** (56 mg, 52%). LCMS (ESI^+): m/z 386.3 $[\text{M} + \text{H}]^+$, rt 1.24 min, >99%; ^1H NMR: (500 MHz, CDCl_3) 7.64 (1H, d, $J = 8.3$ Hz), 7.44 (1H, s), 7.30–7.25 (1H, m), 7.23 (2H, d, $J = 8.1$ Hz), 7.14 (1H, d, $J = 3.2$ Hz), 7.03 (2H, d, $J = 8.2$ Hz), 6.54 (1H, dd, $J = 3.1, 0.7$ Hz), 5.88 (1H, s), 5.27 (2H, s), 3.68 (2H, br s), 3.41 (2H, s), 2.33 (4H, br s), 1.58–1.50 (4H, m), 1.45–1.36 (2H, m); ^{13}C NMR: (125 MHz, CDCl_3) 155.1 (br), 146.6 (br), 138.4, 136.6, 135.8, 129.8, 129.7, 129.1, 126.7, 123.9, 121.6,

117.7, 106.8, 102.0, 90.6, 63.5, 54.6, 50.0, 26.0, 24.4; $\nu_{\text{max}}/\text{cm}^{-1}$: 2926, 2848, 2789, 2757, 1586, 1505; HRMS (ESI^+): m/z calcd for $[\text{C}_{24}\text{H}_{27}\text{N}_5 + \text{H}]^+$, 386.2339; observed, 386.2336.

Expression and Purification of Full Length *Mab* TrmD. Expression and purification was carried out as previously described.¹² AVA0421 plasmid with an N-His-3C Protease site-TrmD full-length insert (kindly provided by the Seattle Structural Genomics Consortium) was used for expression. *E. coli* BL21 (DE3) strain containing the above plasmid was grown overnight at 37 °C in 2xYT media, supplemented with ampicillin (100 $\mu\text{g}/\text{mL}$), until optical density ($A_{600\text{nm}}$) reached 0.6. The expression of recombinant construct was induced by the addition of isopropyl β -D-1-thiogalactopyranoside (IPTG) to a final concentration of 0.5 mM and further allowed to grow at 18 °C for 16 h. Cells were harvested by centrifugation at 4 °C for 20 min at 5000g and the pellet re-suspended in buffer A [25 mM 4-(2-hydroxyethyl)-1-piperazineethanesulfonic acid (HEPES) pH 7.5, 500 mM NaCl, 5% glycerol, 10 mM MgCl_2 , 1 mM tris(2-carboxyethyl)-phosphine (TCEP), 20 mM imidazole]. 0.1% Triton (Sigma), 10 $\mu\text{g}/\text{mL}$ DNaseI, 5 mM MgCl_2 , and 3 protease inhibitor cocktail tablets (New England Biolabs) were added to the cell suspension. The clarified cell lysate was filtered using a 0.45 μm syringe filter and passed through a pre-equilibrated (with buffer A), 10 mL pre-packed nickel-sepharose column (HiTrap IMAC FF, GE Healthcare). The column was washed with buffer A and the bound protein eluted using buffer B (25 mM HEPES pH 7.5, 500 mM NaCl, 5% glycerol, 1 mM TCEP, 500 mM imidazole). 3C Protease was added to the pooled elutes and subjected to dialysis, against 2 L of buffer C (25 mM HEPES pH 7.5, 500 mM NaCl, 5% glycerol, 1 mM TCEP) overnight at 4 °C, to cleave the His-tag. The dialyzed protein was then passed through a pre-equilibrated (buffer A) 5 mL HiTrap IMAC FF Nickel column (GE Healthcare). The flow through from the column was collected and concentrated to 3 mL using a 10 kDa centrifugal concentrator (Sartorius Stedim) and loaded onto a pre-equilibrated (with buffer D: 25 mM HEPES pH 7.5, 500 mM NaCl, 5% glycerol) 120 mL Superdex200 16/600 column (GE Healthcare), and 2 mL fractions were collected and analyzed on a 15% SDS-PAGE gel and by MALDI fingerprinting.

Soaking and Co-crystallization of *Mab* TrmD with Fragments and Compounds. Experiments for SAM, **1**, **16**, **20**, **23**, **24f**, **26f**, **29a**, **29d**, and **31a** have been described.¹² Soaking experiments with the remaining compounds were performed as previously described.¹² *Mab* TrmD apo crystals were grown at 19 °C in 48-well sitting drop plates (Swiss CDI) using 0.08 mM sodium cacodylate pH 6.5–7.0, 1–2 M ammonium sulfate and 20 mg/mL of the protein in storage buffer (25 mM HEPES pH 7.5, 500 mM NaCl, 5% glycerol) at drop ratio 1 $\mu\text{L}/1$ μL (protein: reservoir respectively) and equilibrated against 250 μL reservoir solution. The apo crystals formed were allowed to soak in a 4 μL drop containing reservoir solution and 10 mM compound (in DMSO) and equilibrated against 700 μL of the corresponding reservoir solution overnight at 19 °C in 24-well hanging drop vapor diffusion plates.

X-ray Data Collection and Processing. The *Mab* TrmD crystals were cryo-cooled in mother liquor containing 27.5% ethylene glycol. Crystallographic data collection and processing was performed as previously described.¹² X-ray data sets were collected on I04, I03, I02, I04-1, or I24 beamlines at the Diamond Light Source (UK), using the rotation method at a wavelength of 0.979 Å, omega start: 0°, omega oscillation: 0.1°–0.2°, total images: 2100–2400, exposure time: 0.05–0.08 s. The diffraction images were processed using AutoPROC, utilizing XDS for indexing, integration, followed by POINTLESS, AIMLESS and TRUNCATE programs from CCP4 Suite for data reduction, scaling, and the calculation of structure factor amplitudes and intensity statistics.^{33–38}

Mab TrmD ligand-bound structures were solved by molecular replacement using PHASER with the atomic coordinates of the solved *Mab* TrmD apo structure (PDB code 6NVR) as a search model.³⁹ Structure refinement was carried out using REFMAC and PHE-NIX.^{40,41} The models obtained were manually re-built using the COOT interactive graphics program and electron density maps calculated with $2|F_o| - |F_c|$ and $|F_o| - |F_c|$ coefficients.^{42,43} Positions of ligands and water molecules were located in difference electron density maps, and OMIT

difference maps $|mF_o - DF_c|$ were calculated and analyzed to further verify positions of ligands.⁴⁴

Differential Scanning Fluorimetry. Experiments for fragments 1, 16–18, and 20–21 at 5 mM concentration have been described.¹² DSF was performed using a BioRad CFX Connect system, from 25 to 95 °C in 0.5 °C increments of 30 s duration. Samples were run in 96-well plates, with each well containing a final volume of 25 μ L. Screening was conducted with 50 mM HEPES pH 7.5, 500 mM NaCl, 5x SyproOrange, 10 μ M *Mab* TrmD, and either 5% DMSO or 5% ligand stock solution in DMSO.

Isothermal Titration Calorimetry. Experiments for 16, 20, 23, 24f, 26f, 28, 29a, 29d, and 31a have been described.¹² ITC experiments with the remaining compounds to quantify binding to *Mab* TrmD were performed as previously described,¹² using Malvern MicroCal iTC200 or Auto-iTC200 systems at 25 °C. Titrations consisted of an initial injection (0.2 μ L), discarded during data processing, followed by either 19 (2 μ L) or 39 (1 μ L) injections separated by intervals of 60–150 s duration. Protein was dialyzed overnight at 4 °C in storage buffer (50 mM HEPES pH 7.5, 500 mM NaCl, 5% glycerol). Sample cell and syringe solutions were prepared using the same storage buffer, with a final DMSO concentration of 2–10% according to ligand solubility in the buffer. TrmD concentrations of either 33 or 100 μ M were used, with ligand to protein concentration ratios ranging from 10 to 20:1. Control titrations without protein were also performed and subtracted from ligand to protein titrations. Titrations were fitted with Origin software (OriginLab, Northampton, MA, USA), using a one-site binding model with N fixed to 1 only for weakly binding ligands. Titrations were typically performed once ($n = 1$), with multiple isotherms obtained ($n > 1$) for key compounds of interest. K_d values are reported to 2 significant figures. Error provided by Origin software due to model fit is reported when $n = 1$, whereas standard deviation is reported when $n > 1$.

For the reverse ITC titration with 26o (Figure S8b), protein solution (420 μ M TrmD) was injected into the sample cell (35 μ M ligand). Other aspects of the experiment setup and analysis were identical to the forward titrations.

Native Mass Spectrometry. Native nano-electrospray ionization mass spectrometry spectra were recorded on a Synapt HDMS mass spectrometer (Waters, Manchester, UK) modified for studying high masses. *Mab* TrmD was exchanged into 200 mM ammonium acetate (pH 7.0) solution using Micro Bio-Spin 6 chromatography columns (Bio-Rad, UK). Protein samples were equilibrated at room temperature in the absence or presence of the indicated concentrations of ligands for at least 15 min before analysis. Protein solution (2.5 μ L) was injected into a gold-coated borosilicate emitter (Thermo Scientific, UK) for sampling. Typical conditions were capillary voltage 1.5 kV, cone voltage 50 V, trap collision voltage 20 V, transfer collision voltage 20 V, source temperature 20 °C, backing pressure 3–4 mbar, trap pressure 3–4 $\times 10^{-2}$ mbar, IM (N_2) pressure 5–6 $\times 10^{-1}$ mbar and TOF pressure 7–8 $\times 10^{-7}$ mbar. All mass spectra were calibrated externally with caesium iodide (10 mg/mL). Data acquisition and processing were performed using MassLynx 4.1 (Waters).

Screening against *Mab*. *Mab* subspecies *abscessus* (ATCC 19977) was transformed with pmv310 plasmid expressing Lux ABDCE operon, grown in Middlebrook 7H9 broth supplemented with ADC (Sigma, UK). Minimum Inhibitory Concentrations (MIC) were determined according to the Clinical and Laboratory Standards Institute (CLSI) method M07-A9. Mycobacteria were grown to an OD₆₀₀ of 0.2–0.3 in liquid culture, and 1 $\times 10^8$ bacteria were added to each well of 96-well plates containing serial dilutions of compound (400, 200, 100, 50, 25, 12.5, 6.3, 3.1, 1.6, 0.8, 0.4, 0 μ M), in triplicate wells per condition, and incubated at 37 °C until growth was seen in the control wells. The MIC value was determined as the last well which showed no bacterial growth.

Screening against H37Rv *Mtb*. Antimicrobial susceptibility testing against *Mtb* H37Rv was performed in various media including: GAST-Fe, 7H9/ADC, 7H9/DPPC (4.7 g/L 7H9 base, 14 mg/L DPPC, 0.81 g/L NaCl, 0.3 g/L Casitone, and 0.05% Tyloxapol), and 7H9/Glucose (4.7 g/L 7H9 base, 4 g/L glucose, 0.81 g/L NaCl, 0.3 g/L Casitone, and 0.05% Tyloxapol). H37Rv was grown in the corresponding media to OD 0.2–0.4 prior to use. A two-fold serial dilution series (50 μ L) was placed in each well of a sterile 96-well round

bottom plate, and then 50 μ L of H37Rv diluted to OD 0.0002 was added. Plates were incubated at 37 °C for 2 weeks prior to determining MIC. The MIC is defined here as the drug concentration that completely inhibits growth of cells.

■ ASSOCIATED CONTENT

📄 Supporting Information

The Supporting Information is available free of charge on the ACS Publications website at DOI: 10.1021/acs.jmedchem.9b00809.

Synthesis of intermediates, X-ray crystal structures of *Mab* TrmD in complex with compounds 3, 8, and 14, X-ray crystal structures of *Mab* TrmD in complex with compounds 22, 24d, 26n, and 31b, X-ray crystallographic data collection and refinement statistics, and ITC traces (PDF)

Molecular formula strings (CSV)

Accession Codes

Atomic coordinates for the X-ray structures of compounds 1 (PDB code 6NW6), 3 (PDB code 6QRF), 7 (PDB code 6QRE), 8 (PDB code 6QRG), 14 (PDB code 6QQQ), 16 (PDB Code 6QOT), 20 (PDB code 6QOU), 22 (PDB code 6QQR), 23 (PDB code 6QQS), 24a (PDB code 6QQT), 24b (PDB code 6QRC), 24c (PDB code 6QQW), 24d (PDB code 6QQV), 24f (PDB code 6QQX), 25 (PDB code 6QQU), 26f (PDB code 6QQY), 26g (PDB code 6QQZ), 26n (PDB code 6QR4), 27g (PDB code 6QR1), 26j (PDB code 6QR2), 26l (PDB code 6QR0), 26o (PDB code 6QR3), 29a (PDB code 6QR6), 29b (PDB code 6QR7), 29c (PDB code 6QR9), 29d (PDB code 6QR8), 29e (PDB code 6QRD), 31b (PDB code 6QRA) are available from the RCPB Protein Data Bank (www.rcpb.org). Authors will release the atomic coordinates and experimental data upon article publication.

■ AUTHOR INFORMATION

Corresponding Authors

*E-mail: ca26@cam.ac.uk (C.A.).

*E-mail: tom@cryst.bioc.cam.ac.uk (T.L.B.).

*E-mail: agc40@cam.ac.uk (A.G.C.).

ORCID

M. Daben J. Libardo: 0000-0003-0037-7812

Vitor Mendes: 0000-0002-2734-2444

Helena I. M. Boshoff: 0000-0002-4333-206X

Chris Abell: 0000-0001-9174-1987

Anthony G. Coyne: 0000-0003-0205-5630

Author Contributions

A.J.W. and S.E.T. contributed equally. The manuscript was written through contributions of all authors. All authors have given approval to the final version of the manuscript.

Funding

A.J.W. is funded by the EPSRC; SET is funded by the Cystic Fibrosis Trust and Foundation Botnar; V.M. is funded by the Bill and Melinda Gates Foundation SHORTEN-TB (OPP1158806); T.L.B. is funded by the Wellcome Trust (Wellcome Trust Investigator Award 200814_Z_16_Z); R.A.F. is funded by the Cystic Fibrosis Trust Strategic Research Centre (SRC010) and Innovation Hub (IH01) awards, Wellcome Trust (107032AIA), and Royal Papworth Hospital Research Award. This work was funded in part by the Intramural Research Program of NIH, NIAID (AI000693-25).

Notes

The authors declare no competing financial interest.

ACKNOWLEDGMENTS

The authors would like to thank Dr Glyn Williams for his advice on ITC and Dr Sitthivut Charoensutthivarakul for the collection of HRMS data. The authors would like to thank the Seattle Structural Genomics Consortium for kindly providing the *Mab* trmD AVA0421 plasmid, Diamond Light Source for beam-time (proposals mx9537, mx14043, mx18548) and the staff of beamlines I03, I02, I04, I04-1 and I24 for assistance with data collection.

ABBREVIATIONS

ΔT_m , change in melting temperature; CF, cystic fibrosis; DPPC, dipalmitoyl phosphatidylcholine; DSF, differential scanning fluorimetry; ESI, electrospray ionization; GE, group efficiency; ITC, isothermal titration calorimetry; K_d , binding affinity; LE, ligand efficiency; *Mab*, *Mycobacterium abscessus*; *Mtb*, *Mycobacterium tuberculosis*; MIC, minimum inhibitory concentration; native MS, native mass spectrometry; SAM, S-adenosyl methionine; TrmD, tRNA (m¹G37) methyltransferase

REFERENCES

- (1) Bryant, J. M.; Grogono, D. M.; Rodriguez-Rincon, D.; Everall, I.; Brown, K. P.; Moreno, P.; Verma, D.; Hill, E.; Drijkoningen, J.; Gilligan, P.; Esther, C. R.; Noone, P. G.; Giddings, O.; Bell, S. C.; Thomson, R.; Wainwright, C. E.; Coulter, C.; Pandey, S.; Wood, M. E.; Stockwell, R. E.; Ramsay, K. A.; Sherrard, L. J.; Kidd, T. J.; Jabbar, N.; Johnson, G. R.; Knibbs, L. D.; Morawska, L.; Sly, P. D.; Jones, A.; Bilton, D.; Laurenson, I.; Ruddy, M.; Bourke, S.; Bowler, I. C. J. W.; Chapman, S. J.; Clayton, A.; Cullen, M.; Dempsey, O.; Denton, M.; Desai, M.; Drew, R. J.; Edenborough, F.; Evans, J.; Folb, J.; Daniels, T.; Humphrey, H.; Isalska, B.; Jensen-Fangel, S.; Jönsson, B.; Jones, A. M.; Katzenstein, T. L.; Lillebaek, T.; MacGregor, G.; Mayell, S.; Millar, M.; Modha, D.; Nash, E. F.; O'Brien, C.; O'Brien, D.; Ohri, C.; Pao, C. S.; Peckham, D.; Perrin, F.; Perry, A.; Pressler, T.; Prtak, L.; Qvist, T.; Robb, A.; Rodgers, H.; Schaffer, K.; Shafi, N.; van Ingen, J.; Walshaw, M.; Watson, D.; West, N.; Whitehouse, J.; Haworth, C. S.; Harris, S. R.; Ordway, D.; Parkhill, J.; Floto, R. A. Emergence and spread of a human-transmissible multidrug-resistant nontuberculous mycobacterium. *Science* **2016**, *354*, 751–757.
- (2) Haworth, C. S.; Banks, J.; Capstick, T.; Fisher, A. J.; Gorsuch, T.; Laurenson, I. F.; Leitch, A.; Loebinger, M. R.; Milburn, H. J.; Nightingale, M.; Ormerod, P.; Shingadia, D.; Smith, D.; Whitehead, N.; Wilson, R.; Floto, R. A. British Thoracic Society guidelines for the management of non-tuberculous mycobacterial pulmonary disease (NTM-PD). *Thorax* **2017**, *72*, ii1–ii64.
- (3) Esther, C. R., Jr; Esserman, D. A.; Gilligan, P.; Kerr, A.; Noone, P. G. Chronic *Mycobacterium abscessus* infection and lung function decline in cystic fibrosis. *J. Cystic Fibrosis* **2010**, *9*, 117–123.
- (4) Qvist, T.; Taylor-Robinson, D.; Waldmann, E.; Olesen, H. V.; Hansen, C. R.; Mathiesen, I. H.; Høiby, N.; Katzenstein, T. L.; Smyth, R. L.; Diggle, P. J.; Pressler, T. Comparing the harmful effects of nontuberculous mycobacteria and gram negative bacteria on lung function in patients with cystic fibrosis. *J. Cystic Fibrosis* **2016**, *15*, 380–385.
- (5) Floto, R. A.; Olivier, K. N.; Saiman, L.; Daley, C. L.; Herrmann, J.-L.; Nick, J. A.; Noone, P. G.; Bilton, D.; Corris, P.; Gibson, R. L.; Hempstead, S. E.; Koetz, K.; Sabadosa, K. A.; Sermet-Gaudelus, I.; Smyth, A. R.; van Ingen, J.; Wallace, R. J.; Winthrop, K. L.; Marshall, B. C.; Haworth, C. S. US Cystic Fibrosis Foundation and European Cystic Fibrosis Society consensus recommendations for the management of non-tuberculous mycobacteria in individuals with cystic fibrosis. *Thorax* **2016**, *71*, i1–i22.
- (6) Nessar, R.; Cambau, E.; Reyrat, J. M.; Murray, A.; Gicquel, B. *Mycobacterium abscessus*: a new antibiotic nightmare. *J. Antimicrob. Chemother.* **2012**, *67*, 810–818.
- (7) Goto-Ito, S.; Ito, T.; Yokoyama, S. TrmS and TrmD: Two Enzymes from Distinct Origins Catalyze the Identical tRNA Modification, m1G37. *Biomolecules* **2017**, *7*, 32.
- (8) Gamper, H. B.; Masuda, I.; Frenkel-Morgenstern, M.; Hou, Y.-M. Maintenance of protein synthesis reading frame by EF-P and m1G37-tRNA. *Nat. Commun.* **2015**, *6*, 7226.
- (9) Forsyth, R. A.; Haselbeck, R. J.; Ohlsen, K. L.; Yamamoto, R. T.; Xu, H.; Trawick, J. D.; Wall, D.; Wang, L.; Brown-Driver, V.; Froelich, J. M.; King, P.; McCarthy, M.; Malone, C.; Misiner, B.; Robbins, D.; Tan, Z.; Zhu, Z.-y.; Carr, G.; Mosca, D. A.; Zamudio, C.; Foulkes, J. G.; Zyskind, J. W. A genome-wide strategy for the identification of essential genes in *Staphylococcus aureus*. *Mol. Microbiol.* **2002**, *43*, 1387–1400.
- (10) Turner, K. H.; Wessel, A. K.; Palmer, G. C.; Murray, J. L.; Whiteley, M. Essential genome of *Pseudomonas aeruginosa* in cystic fibrosis sputum. *Proc. Natl. Acad. Sci. U.S.A.* **2015**, *112*, 4110–4115.
- (11) Sasseti, C. M.; Boyd, D. H.; Rubin, E. J. Genes required for mycobacterial growth defined by high density mutagenesis. *Mol. Microbiol.* **2003**, *48*, 77–84.
- (12) Thomas, S. E.; Whitehouse, A. J.; Brown, K.; Belardinelli, J. M.; Lahiri, R.; Libardo, M. D. J.; Gupta, P.; Malhotra, S.; Boshoff, H. I. M.; Jackson, M.; Abell, C.; Coyne, A. G.; Blundell, T. L.; Floto, R. A.; Mendes, V. Fragment-based Discovery of a New Class of Inhibitors Targeting Mycobacterial tRNA Modification. 2019, arXiv: 564013, DOI: <https://doi.org/10.1101/564013>, <https://www.biorxiv.org/content/10.1101/564013v1> (accessed May 09, 2019).
- (13) Baugh, L.; Phan, I.; Begley, D. W.; Clifton, M. C.; Armour, B.; Dranow, D. M.; Taylor, B. M.; Muruthi, M. M.; Abendroth, J.; Fairman, J. W.; Fox, D., III; Dieterich, S. H.; Staker, B. L.; Gardberg, A. S.; Choi, R.; Hewitt, S. N.; Napuli, A. J.; Myers, J.; Barrett, L. K.; Zhang, Y.; Ferrell, M.; Mundt, E.; Thompkins, K.; Tran, N.; Lyons-Abbott, S.; Abramov, A.; Sekar, A.; Serbzhinskiy, D.; Lorimer, D.; Buchko, G. W.; Stacy, R.; Stewart, L. J.; Edwards, T. E.; Van Voorhis, W. C.; Myler, P. J. Increasing the structural coverage of tuberculosis drug targets. *Tuberculosis* **2015**, *95*, 142–148.
- (14) Elkins, P. A.; Watts, J. M.; Zalacain, M.; van Thiel, A.; Vitazka, P. R.; Redlak, M.; Andraos-Selim, C.; Rastinejad, F.; Holmes, W. M. Insights into catalysis by a knotted TrmD tRNA methyltransferase. *J. Mol. Biol.* **2003**, *333*, 931–949.
- (15) Ahn, H. J.; Kim, H.-W.; Yoon, H.-J.; Lee, B. I.; Suh, S. W.; Yang, J. K. Crystal structure of tRNA(m1G37)methyltransferase: Insights into tRNA recognition. *EMBO J.* **2003**, *22*, 2593–2603.
- (16) Ito, T.; Masuda, I.; Yoshida, K.-i.; Goto-Ito, S.; Sekine, S.-i.; Suh, S. W.; Hou, Y.-M.; Yokoyama, S. Structural basis for methyl-donor-dependent and sequence-specific binding to tRNA substrates by knotted methyltransferase TrmD. *Proc. Natl. Acad. Sci. U.S.A.* **2015**, *112*, E4197–E4205.
- (17) Goto-Ito, S.; Ito, T.; Kuratani, M.; Bessho, Y.; Yokoyama, S. Tertiary structure checkpoint at anticodon loop modification in tRNA functional maturation. *Nat. Struct. Mol. Biol.* **2009**, *16*, 1109–1115.
- (18) Zhong, W.; Koay, A.; Ngo, A.; Li, Y.; Nah, Q.; Wong, Y. H.; Chionh, Y. H.; Ng, H. Q.; Koh-Stenta, X.; Poulsen, A.; Foo, K.; McBee, M.; Choong, M. L.; El Sahili, A.; Kang, C.; Matter, A.; Lescar, J.; Hill, J.; Dedon, P. Targeting the bacterial epitranscriptome for antibiotic development: Discovery of novel tRNA-(N1G37) methyltransferase (TrmD) inhibitors. *ACS Infect. Dis.* **2019**, *5*, 326–335.
- (19) Scott, D. E.; Coyne, A. G.; Hudson, S. A.; Abell, C. Fragment-based approaches in drug discovery and chemical biology. *Biochemistry* **2012**, *51*, 4990–5003.
- (20) Hill, P. J.; Abibi, A.; Albert, R.; Andrews, B.; Gagnon, M. M.; Gao, N.; Grebe, T.; Hajec, L. I.; Huang, J.; Livchak, S.; Lahiri, S. D.; McKinney, D. C.; Thresher, J.; Wang, H.; Olivier, N.; Buurman, E. T. Selective Inhibitors of Bacterial tRNA-(N1G37) Methyltransferase (TrmD) That Demonstrate Novel Ordering of the Lid Domain. *J. Med. Chem.* **2013**, *56*, 7278–7288.

- (21) Lundbäck, T.; O'Brien, R.; Williams, G. *The Mix: Simultaneous Affinity Determination for Isomers and Enantiomers*; MicroCal: Northampton, MA, USA, 2006.
- (22) Hernández, H.; Robinson, C. V. Determining the stoichiometry and interactions of macromolecular assemblies from mass spectrometry. *Nat. Protoc.* **2007**, *2*, 715–726.
- (23) Chan, D. S.-H.; Matak-Vinković, D.; Coyne, A. G.; Abell, C. Insight into protein conformation and subcharging by DMSO from native ion mobility mass spectrometry. *ChemistrySelect* **2016**, *1*, 5686–5690.
- (24) Sterling, H. J.; Prell, J. S.; Cassou, C. A.; Williams, E. R. Protein conformation and supercharging with DMSO from aqueous solution. *J. Am. Soc. Mass Spectrom.* **2011**, *22*, 1178–1186.
- (25) Zanaletti, R.; Bettinetti, L.; Castaldo, C.; Cocconcelli, G.; Comery, T.; Dunlop, J.; Gaviraghi, G.; Ghiron, C.; Haydar, S. N.; Jow, F.; Maccari, L.; Micco, I.; Nencini, A.; Scali, C.; Turlizzi, E.; Valacchi, M. Discovery of a Novel Alpha-7 Nicotinic Acetylcholine Receptor Agonist Series and Characterization of the Potent, Selective, and Orally Efficacious Agonist 5-(4-Acetyl[1,4]diazepan-1-yl)pentanoic Acid [5-(4-Methoxyphenyl)-1H-pyrazol-3-yl] Amide (SEN15924, WAY-361789). *J. Med. Chem.* **2012**, *55*, 4806–4823.
- (26) Hassaneen, H. M. E. New Approach to 4- and 5-Aminopyrazole Derivatives. *Synth. Commun.* **2007**, *37*, 3579–3588.
- (27) Wender, P. A.; Beckham, S.; O'Leary, J. G. A second generation photochemically activatable dynemicin analog: A concise synthesis and DNA cleavage studies. *Synthesis* **1994**, *1994*, 1278–1282.
- (28) Soni, A.; Dutt, A.; Sattigeri, V.; Cliffe, I. A. Efficient and selective demethylation of heteroaryl methyl ethers in the presence of aryl methyl ethers. *Synth. Commun.* **2011**, *41*, 1852–1857.
- (29) Soler, M.; Figueras, E.; Serrano-Plana, J.; González-Bártulos, M.; Massaguer, A.; Company, A.; Martínez, M. A.; Malina, J.; Brabec, V.; Feliu, L.; Planas, M.; Ribas, X.; Costas, M. Design, preparation, and characterization of Zn and Cu metallopeptides based on tetradentate aminopyridine ligands showing enhanced DNA cleavage activity. *Inorg. Chem.* **2015**, *54*, 10542–10558.
- (30) Deb, I.; Das, D.; Seidel, D. Redox Isomerization via Azomethine Ylide Intermediates: N-Alkyl Indoles from Indolines and Aldehydes. *Org. Lett.* **2011**, *13*, 812–815.
- (31) Doebelin, C.; Patouret, R.; Garcia-Ordóñez, R. D.; Chang, M. R.; Dharmarajan, V.; Kuruvilla, D. S.; Novick, S. J.; Lin, L.; Cameron, M. D.; Griffin, P. R.; Kamenecka, T. M. N-Arylsulfonyl Indolines as Retinoic Acid Receptor-Related Orphan Receptor γ (ROR γ) Agonists. *ChemMedChem* **2016**, *11*, 2607–2620.
- (32) Ehrt, S.; Rhee, K. Mycobacterium tuberculosis metabolism and host interaction: mysteries and paradoxes. *Curr. Top Microbiol. Immunol.* **2013**, *374*, 163–188.
- (33) Vonrhein, C.; Flensburg, C.; Keller, P.; Sharff, A.; Smart, O.; Paciorek, W.; Womack, T.; Bricogne, G. Data processing and analysis with the autoPROC toolbox. *Acta Crystallogr., Sect. D: Biol. Crystallogr.* **2011**, *67*, 293–302.
- (34) Kabsch, W. XDS. *Acta Crystallogr., Sect. D: Biol. Crystallogr.* **2010**, *66*, 125–132.
- (35) Evans, P. R. An introduction to data reduction: Space-group determination, scaling and intensity statistics. *Acta Crystallogr., Sect. D: Biol. Crystallogr.* **2011**, *67*, 282–292.
- (36) Evans, P. R.; Murshudov, G. N. How good are my data and what is the resolution? *Acta Crystallogr., Sect. D: Biol. Crystallogr.* **2013**, *69*, 1204–1214.
- (37) French, S.; Wilson, K. On the treatment of negative intensity observations. *Acta Crystallogr., Sect. A: Cryst. Phys., Diffr., Theor. Gen. Crystallogr.* **1978**, *34*, 517–525.
- (38) Winn, M. D.; Ballard, C. C.; Cowtan, K. D.; Dodson, E. J.; Emsley, P.; Evans, P. R.; Keegan, R. M.; Krissinel, E. B.; Leslie, A. G. W.; McCoy, A.; McNicholas, S. J.; Murshudov, G. N.; Pannu, N. S.; Potterton, E. A.; Powell, H. R.; Read, R. J.; Vagin, A.; Wilson, K. S. Overview of the CCP4 suite and current developments. *Acta Crystallogr., Sect. D: Biol. Crystallogr.* **2011**, *67*, 235–242.
- (39) McCoy, A. J.; Grosse-Kunstleve, R. W.; Adams, P. D.; Winn, M. D.; Storoni, L. C.; Read, R. J. Phaser crystallographic software. *J. Appl. Crystallogr.* **2007**, *40*, 658–674.
- (40) Murshudov, G. N.; Skubák, P.; Lebedev, A. A.; Pannu, N. S.; Steiner, R. A.; Nicholls, R. A.; Winn, M. D.; Long, F.; Vagin, A. A. REFMAC5 for the refinement of macromolecular crystal structures. *Acta Crystallogr., Sect. D: Biol. Crystallogr.* **2011**, *67*, 355–367.
- (41) Adams, P. D.; Afonine, P. V.; Bunkóczi, G.; Chen, V. B.; Davis, I. W.; Echols, N.; Headd, J. J.; Hung, L.-W.; Kapral, G. J.; Grosse-Kunstleve, R. W.; McCoy, A. J.; Moriarty, N. W.; Oeffner, R.; Read, R. J.; Richardson, D. C.; Richardson, J. S.; Terwilliger, T. C.; Zwart, P. H. PHENIX: A comprehensive Python-based system for macromolecular structure solution. *Acta Crystallogr., Sect. D: Biol. Crystallogr.* **2010**, *66*, 213–221.
- (42) Emsley, P.; Cowtan, K. Coot: Model-building tools for molecular graphics. *Acta Crystallogr., Sect. D: Biol. Crystallogr.* **2004**, *60*, 2126–2132.
- (43) Emsley, P.; Lohkamp, B.; Scott, W. G.; Cowtan, K. Features and development of Coot. *Acta Crystallogr., Sect. D: Biol. Crystallogr.* **2010**, *66*, 486–501.
- (44) Hodel, A.; Kim, S. H.; Brünger, A. T. Model bias in macromolecular crystal structures. *Acta Crystallogr., Sect. A: Found. Crystallogr.* **1992**, *48*, 851–858.